FLUVIAL TO MARINE FACIES SUCCESSION IN A COMPOUND INCISED VALLEY SYSTEM IN THE FERRON-NOTOM DELTA, UTAH

A Thesis

Presented to

the Faculty of the Department of Earth and Atmospheric Sciences
University of Houston

In Partial Fulfillment

of the Requirements for the Degree

Master of Science

By

Benjamin H. Richards

August 2014

FLUVIAL TO MARINE FACIES SUCCESSION IN A COMPOUND INCISED VALLEY SYSTEM IN THE FERRON-NOTOM DELTA, UTAH

____

Benjamin H. Richards

APPROVED:

____

Dr. Ian Evans, Advisor

____

Dr. Janok P. Bhattacharya, Committee Member

____

Dr. Julia Wellner, Committee Member

____

Dean, College of Natural Science and Mathematics

ACKNOWLEDGEMENTS

I would like to thank my advisor, Dr. Bhattacharya, not only for what I have been taught directly, but also for his high standards and the independence he has encouraged in my work. He endured every question I had for him and responded with careful wording and definitions which have greatly clarified my understanding of geology. I would also like to thank my committee members, Dr. Wellner and Dr. Evans. I could bring ideas to them or meet with them at a moment's notice and their expertise has proven tremendously helpful.

The Quantitative Sedimentology Consortium should be recognized for producing detailed research with real utility. This work is made possible only through their ongoing and generous contributions.

I would also like to thank my colleagues. Oyebode Fambode and Yangyang Li, who allowed me to learn from their experience and enthusiasm in the field. Mohammed Ullah brought me to the field to show me what he knew and discuss geology at length. Proma and Zhiyang and I aided one another wherever possible. I would like to thank Yije Zhu for building an impressive body of work for me to build on.

Finally, I would like to thank both of my parents whose relentless support of my education included, beyond financial support, everything from reading to me as a child to giving me a place I could do my laundry as a graduate student. Any success I may have is, first and foremost, a reflection upon them.

FLUVIAL TO MARINE FACIES SUCCESSION IN A COMPOUND INCISED VALLEY SYSTEM IN THE FERRON-NOTOM DELTA, UTAH

An Abstract of a Thesis

Presented to

the Faculty of the Department of Earth and Atmospheric Sciences
University of Houston

In Partial Fulfillment

of the Requirements for the Degree

Master of Science

By

Benjamin H. Richards

August 2014

ABSTRACT

The Turonian age Ferron sandstone formed in multiple deltas which empty into the Western Interior Seaway, including the Notom delta, which has been shown to contain 6 sequences. A compound incised valley system has been well documented at the base of the youngest sequence 1 in outcrops of the Cretaceous Ferron Notom delta complex in central Utah. That valley was shown to have undergone multiple episodes of cut and fill at high frequency Milankovich scale cyclicity, but correlative marine facies are not exposed. Directly beneath sequence 1, sequence 2 also contains a fluvial valley system. This valley system is particularly well exposed in the most basinward fluvial deposits within parasequence set 6 and can be correlated to coeval marine facies. Previously these deposits had only been documented in regional scale maps and cross sections, and it was interpreted as a single, versus compound valley. This study shows that the older valley is also compound, and more detailed data document the downstream succession of depositional facies comprising the valley fill.

Correlation of 11 measured sections illustrates a basinward increase in tidal facies and reveals distinct lower and upper fluvial valleys, the lower of which feeds a previously documented shoreface facies. This confirms the compound nature of the valley fill in sequence 2. This suggests that the Ferron valleys are compound in nature and correlate with stepped forced regressive shoreline deposits that can be seen in the older shallow-marine strata. This finding demonstrates the importance of non-linear accommodation change in the context of traditional valley fill models.

TABLE OF CONTENTS

LIST OF FIGURES

LIST OF TABLES

1. Introduction

Valley fill deposits can be notoriously complex and can vary temporally, over the course of valley filling, or spatially, from upstream to downstream. It is well established that post-incision transgressions can result in the deposition of tidally influenced valley fill (Fig. 1), but traditional models did not adequately explain the wide variety of valley filling processes (Zaitlin et al., 1994; Korus et al., 2008; Wright et al., 2010 and others). For example, Bhattacharya and Holbrook (2011) suggest that significant bedload sediment may be stored in a valley during falling stage and Li et al. (2011) presented a model for the formation of stepped forced regressive valleys, dominated by falling stage terraces, in the Cretaceous Ferron sandstone of Utah, but these valleys could not be linked to their coeval shallow marine facies.

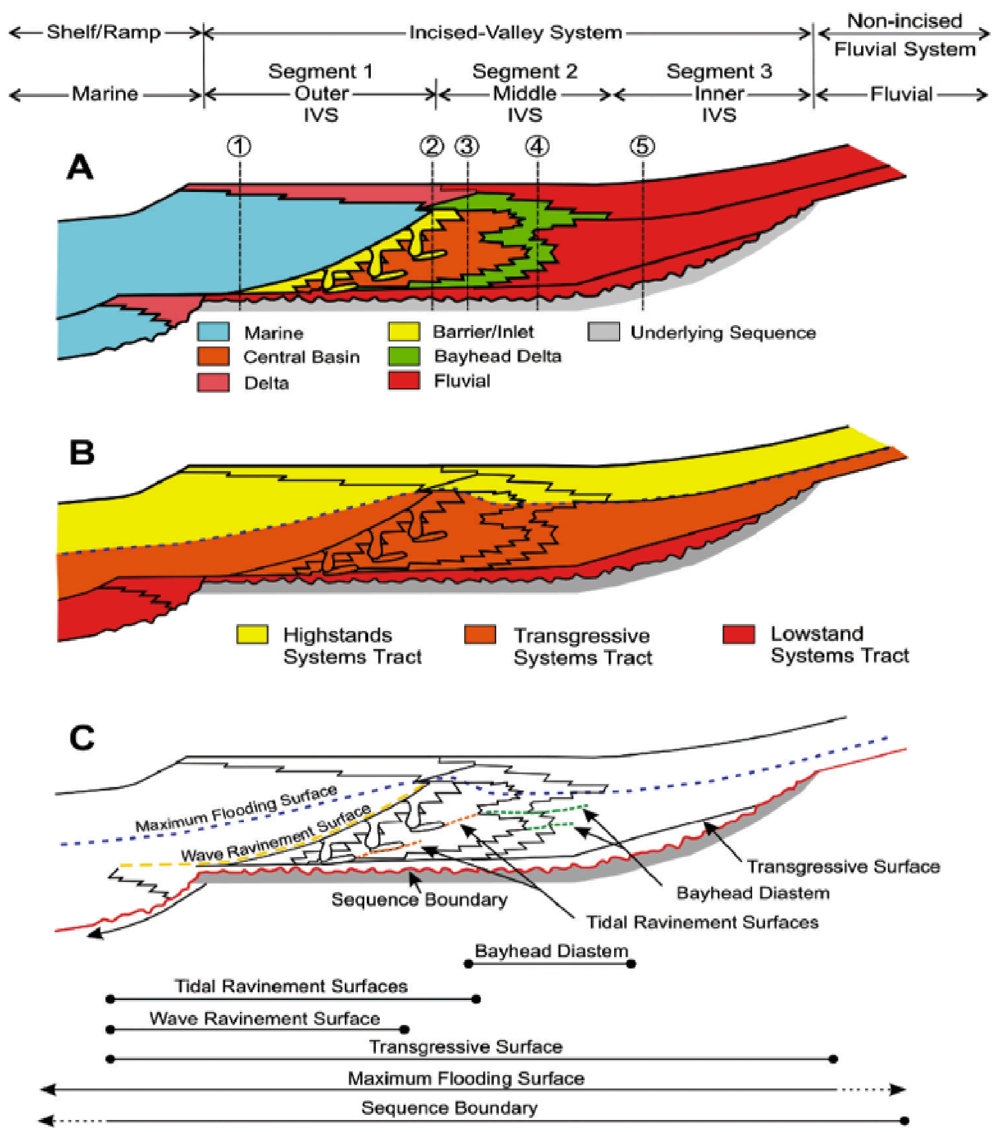

Figure 1: (Zaitlin et al., 1994) Standard model for distribution of depositional environments and facies tracts for valley fills (colorized image from John Holbrook)

Traditional valley models suggest that they are largely cut during the falling stage with the subsequent fill accumulating during the next base-level rise, and contain deposits of the following highstand and subsequent sea-level cycles (Zaitlin et al., 1994; Posamentier, 2001). However, in recent years, several papers (e.g. Bhattacharya, 2011;

Blum et al., 2013) show that valley filling can occur even during accommodation loss (i.e. no complete sediment bypass). Also, modern analogs, in conjunction with some studies of ancient systems, have produced precise measurements of the scale of these systems (Bhattacharya and Tye, 2004) and quantitative analysis of incised valleys can be done by looking at the ratio of incision depth to the depth of the formative channel (Bhattacharya and Tye, 2004). Valley deposits of sufficient thickness may be indicative of a compound valley (Zaitlin et al., 1994). A valley is considered to be compound if it is comprised of an amalgamation of multiple laterally and vertically juxtaposed valleys resulting from multiple episodes of cutting and filling (Zaitlin et al., 1994).

The ancient Ferron sandstone member of the Mancos shale in south-central Utah provides an opportunity to study well-exposed and virtually undeformed valley fill deposits. The regional sequence stratigraphy has already been interpreted (Zhu et al., 2012) and has established six sequences incorporating fluvial and marine strata. Fluvial deposits in the youngest Sequence 1 have already been shown to contain compound incised valleys (Li et al., 2010; Li et al., 2012). To date, the valley fill within Sequence 2 of the Ferron has not been examined in sufficient detail and these rocks, PSS 6 of the Ferron-Notom delta complex outcropping near Caineville, Utah (Fig. 2), have the capacity to enhance our understanding of paleovalley systems in both a local and general context.

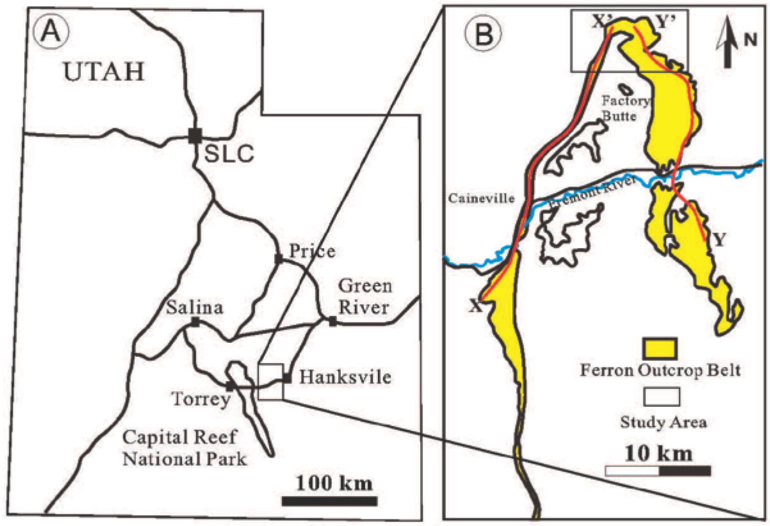

Figure 2: Map of study area. Note the exposures of PSS 6 studied here are just north of Caineville, along the X-X' regional section.

The study of non-marine sequence stratigraphy and fluvial facies architecture both stand to benefit from this research, which provides a detailed, ancient example of intra-valley heterogeneity associated with hypothesized eustatic conditions. The traditional stratigraphic framework for the sequence stratigraphy of fluvial deposits was proposed by Shanely and McCabe (1994) and Wright and Marriott (1993) and these models suggest that base level is the primary control on downstream fluvial stratigraphy. Willis (1997) also stressed the importance of relative sediment supply, in conjunction with base level or accommodation (i.e. supply to accommodation ratio), as a control on valley filling. Specifically, valleys that experience a high sediment supply relative to accommodation increase would have a fluvial fill at their base and would be topped by transgressive or marine facies, thus forming a “flood-topped valley”.

Conversely, valleys that experience rapid accommodation gains relative to sediment supply do not have extensive fluvial deposits at their base and are thus “flood-based” (Willis, 1997).

Recent studies have determined other variables which impact, and potentially enable the prediction of valley filling facies. Blum et al. (2013), for example, emphasizes the impact of the scale of the fluvial valley on its subsequent filling facies. Smaller valley systems are more conducive to the deposition of estuarine facies. Using the discharge of the rivers is a proxy for their size, a “smaller” river example would include the Trinity River, with a discharge of 180 m^3/s whereas the Po River has a discharge of 1540 m^3/s. Li et al. (2010) estimated that fluvial valleys in Sequence 1 of the Ferron-Notom delta had discharges ranging from 390 and 1590 m^3/s. Furthermore, the type and scale of the basin itself impacts the accommodation available and thus affects the aggradation versus erosional tendencies of a given depositional system and foreland basins, such as the Cretaceous Interior Seaway, tend to have sufficient accommodation available to enable sediment aggradation (Blum et al., 2013). The increased accommodation available in the basinward direction also decreases the need for the fluvial profile to degrade and incise in the basinward direction, in other words, valley relief tends to decrease downstream and is correlated with the backwater length of the river. Backwater length is estimated by dividing channel depth by valley slope (Paola and Mohrig, 1996; Blum et al., 2013) and represents the distance over which the bottom of the channel is below sea level, which has a profound impact on deposition. Within backwater lengths, aggradation and avulsion are promoted (Paola and Mohrig, 1996; Blum et al., 2013), thus deeply incised valley systems should have reduced relief in their most distal deposits. Given the steep nature of Ferron fluvial systems with slopes around .001 (Li et al., 2010), a short backwater length of no more than 10 kilometers would be predicated even with a channel depth of 10 meters, which exceeds sequence 1 fluvial depths (Li et al., 2010).

The primary objective of this research is to examine the internal stratigraphy of the valley system within Sequence 2 of the Ferron in order to study the intra-valley variation in facies as well as the extent of tidal influence. In a general sense, this work contributes to the literature on the heterogeneity of valley fills and tests traditional and recent models, while more specifically documenting, in detail, an understudied portion of Sequence 2 of the Ferron.

2. Geologic Setting and Study Area

The Ferron Sandstone is a member of the Cretaceous Mancos Shale and is bounded by the Tununk Shale below and Bluegate Shale above (Fig. 3A, 3B). The Ferron represents the amalgamation of several (fluvio-deltaic) clastic wedges that were deposited on the western edge of the Cretaceous Interior Seaway (Fig. 4) (Ryer and Anderson, 2004). An analog for the Ferron depositional environment can be found at the mouths of the Po (Q_W=1500 M^3/s) and Ebro (Qw = 426 m^3/s) rivers, which are comparable in scale to the Ferron and notably much smaller than well-studied continental scale rivers such as the Mississippi (Qw - 17,000 m^3/s) (Bhattacharya and Tye, 2004). The Ferron Sandstone member contains multiple deltas, including the well-documented Last Chance delta as well as the Vernal delta.

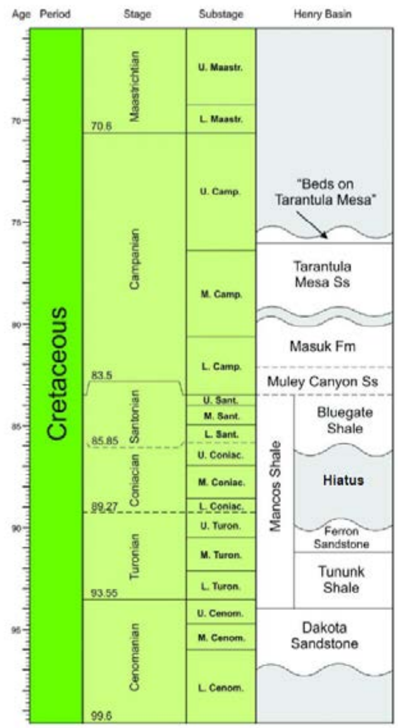

Figure 3A: Large scale stratigraphy of Upper Cretaceous showing the Ferron and its bounding members (from Fielding, 2010)

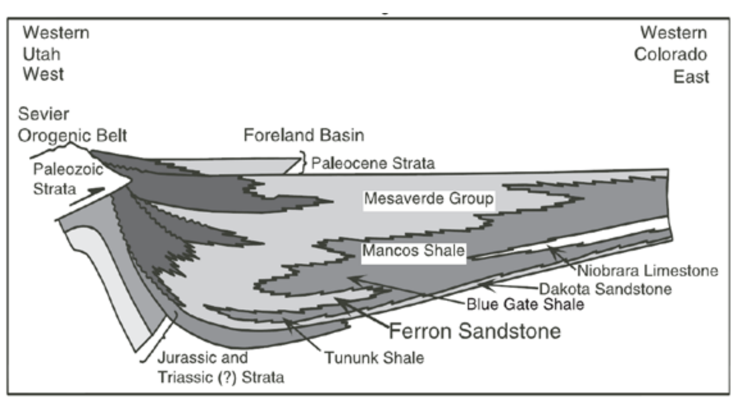

Figure 3B: Local Cretaceous stratigraphy (V3) (after Armstrong, 1968; Ryer, 1981)

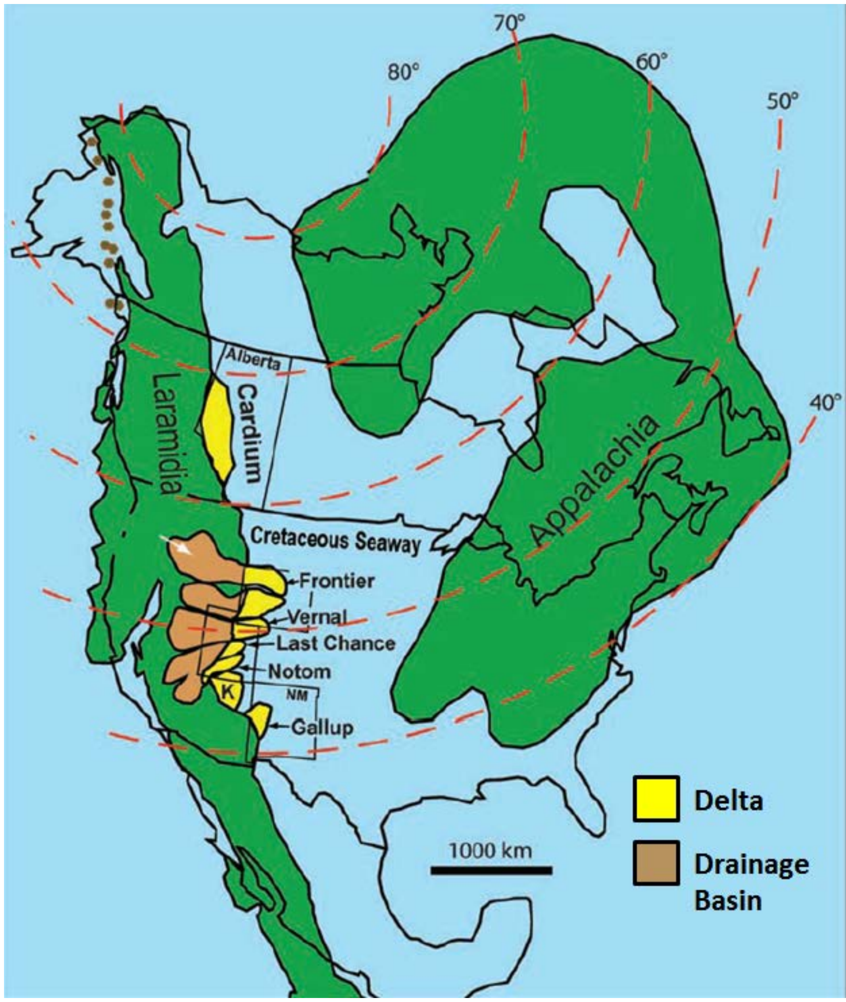

Figure 4: Map of various deltas emptying into the Western Interior Seaway (Bhattacharya and MacEachern, 2009 based on Gardner, 1995)

The delta of interest here is the Notom delta (Fig. 5). The sequence stratigraphy of the Notom system has been interpreted by Li (2009), and Zhu et al. (2012). Bentonite beds have provided material for radiometric dating and have revealed that the Notom formed from 91.2 to 90.6 million years ago (Zhu et al., 2012). There are six depositional sequences that comprise the Notom delta, so each is estimated to have been deposited over approximately 100,000 years (Zhu et al., 2012).

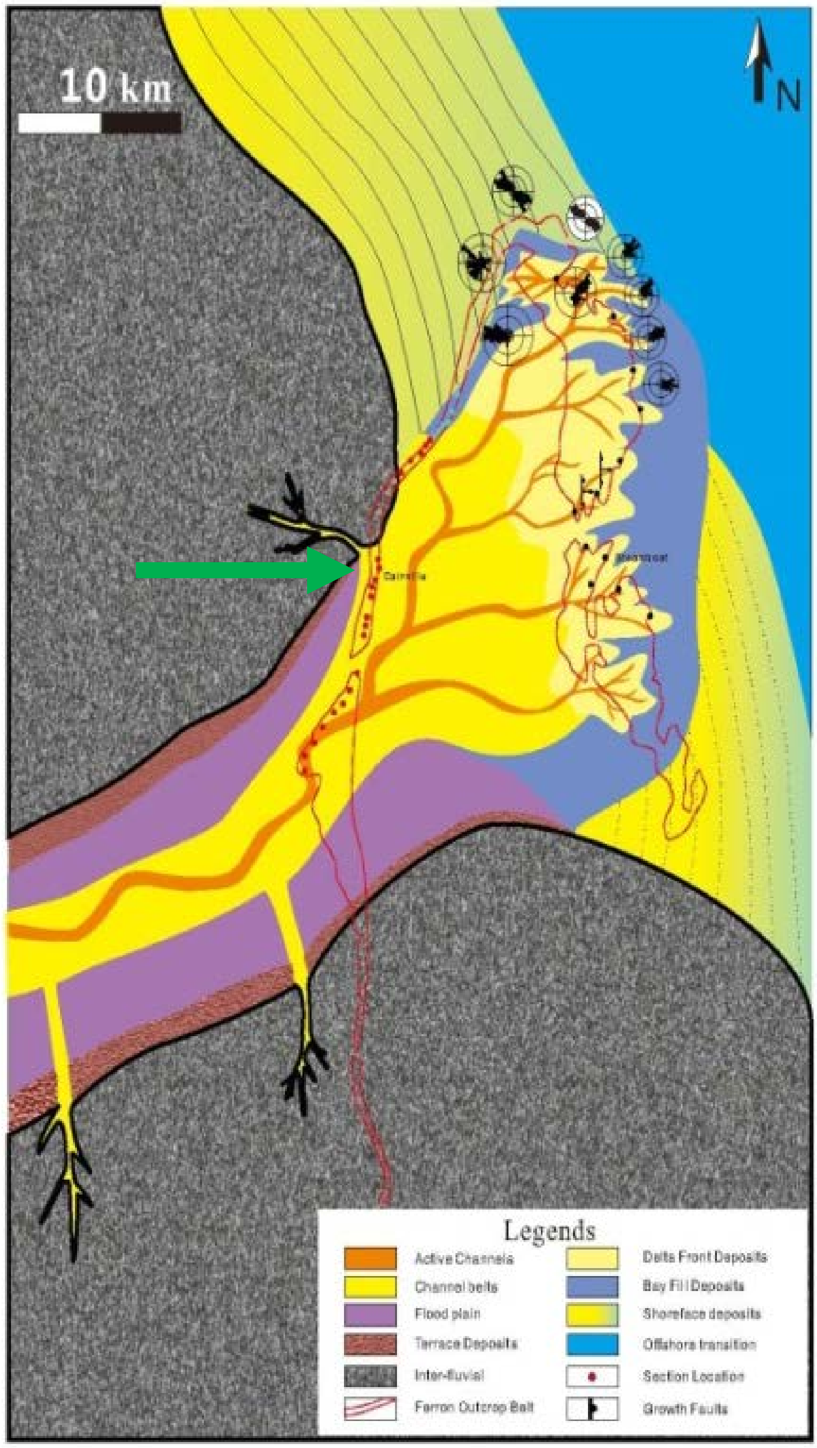

Figure 5: Paleogeographic map of whole Ferron delta for PSS6 (Zhu et al., 2012), Caineville area indicated by green arrow

The Notom delta contains six sequences, which contain a total of 43 parasequences for the entire delta complex (Fig. 6). The youngest of the six sequences, sequence 1, contains multiple compound incised valley systems at its base that are very well exposed (Li et al., 2010; Li and Bhattacharya, 2013) in the Coalmine and Neilson Wash areas. These studies provide data that will be compared with the older incised valleys at the base of sequence 2. Sequence 2 is the first major fluvial sequence in the Notom. Older sequences 3 through 6 contain mostly marine deposits. Previous work on multiple related compound paleovalleys in sequence 1 found that the juxtaposed valleys showed a sharp basinward shift in facies (Li et al., 2010; Li and Bhattacharya, 2013) in conjunction with terrace deposits and sufficiently deep erosion that demonstrate the incised nature of the valleys.

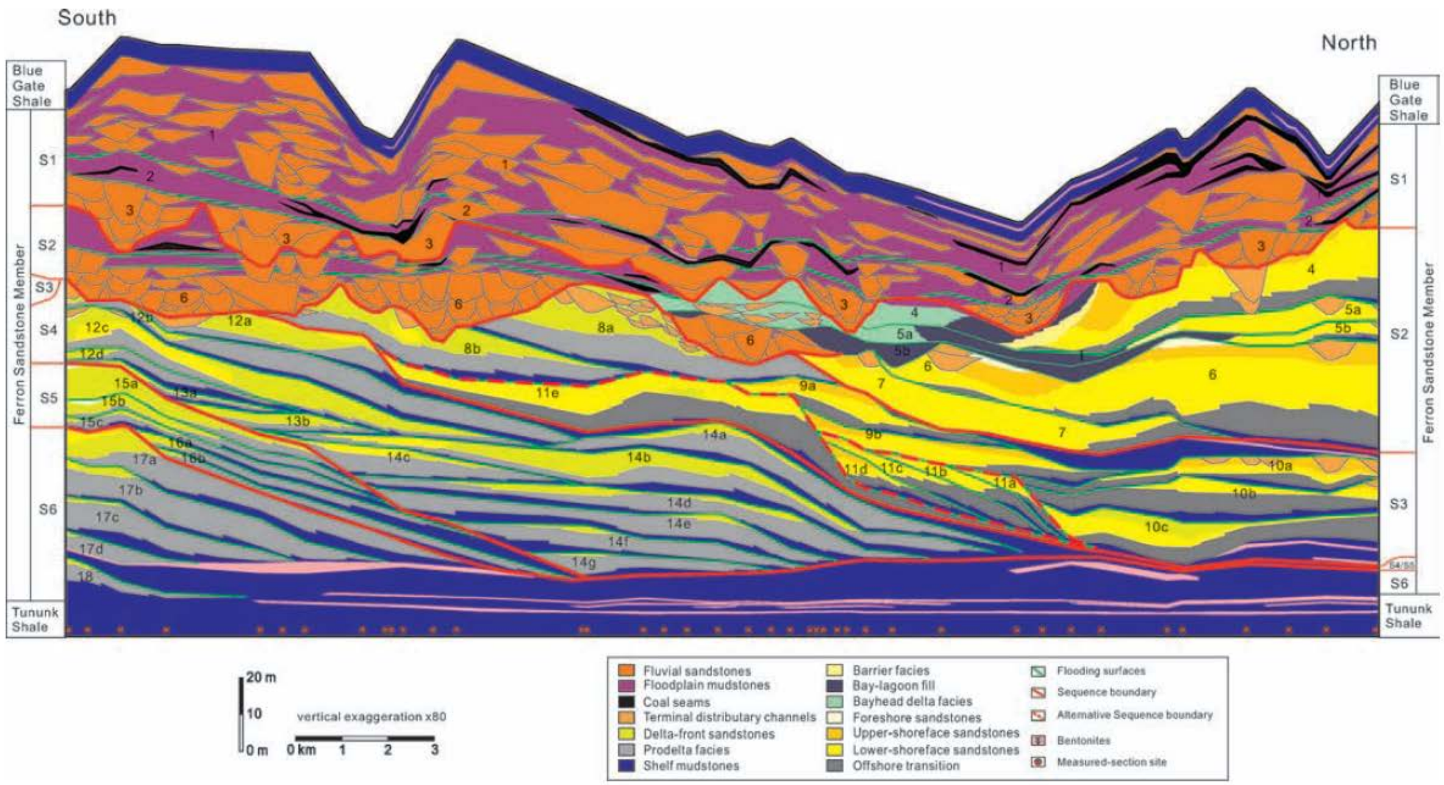

Figure 6: Regional dip cross section, 43 parasequences and 5 sequence boundaries in total, orange fluvial deposits of PSS6 visible (Zhu et al., 2012)

Valley fills can include a variety of deposits ranging from fluvial to open marine (Zaitlin et al., 1994). The fill observed within sequence 1 of the Ferron varies from fluvial to tide-influenced fluvial and estuarine, although no open marine facies were found in Sequence 1 (Li et al., 2010). An incised valley can also be classified as bedrock-alluvial, piedmont, coastal plain, and cross shelf (Boyd, 2006; Blum et al., 2013). The valleys in sequence 1 incise into their own deltaic and coastal-plain facies, suggesting a coastal-plain system. Valley 2 incises into both alluvial, coastal plain and inner-shelf facies and are thus coastal plain to cross-shelf in nature (Zaitlin et al., 1994; Blum et al., 2013). However, the observation of extraformational conglomerate in the valley fills in both sequences suggests that rivers are connected to the hinterland (conveyer belt model) versus localized entirely within the coastal plain (vacuum cleaner model of Blum and Törnqvist, 2000; and Blum et al., 2013 in which the valley itself is the sediment source; as opposed to the conveyor belt model). The valleys are thus linked piedmont and coastal-plain systems.

The Ferron crops out extensively in several areas around southern Utah, and has been reasonably well studied near the town of Hanksville. More specifically, the fluvial portions of sequence 2 are exposed near the town of Caineville, Utah, 30 kilometers west of Hanksville (Fig. 7A, 7B). Strata form a north-south-oriented ridge which dips at a shallow angle (under 30 degrees) to the east, and contain strike and dip exposures that reveal much of the local stratigraphy, including sequence boundary 2 and the overlying strata. Note that the stratigraphy here exhibits minor tilting, unlike most Ferron exposures, due to post-depositional deformation relating to the formation of the San Rafael Swell and the Sevier Orogeny (Van Wagoner, 1995). Fortunately, the exposures studied in the Caineville area have been uniformly affected, thereby minimizing structural complications.

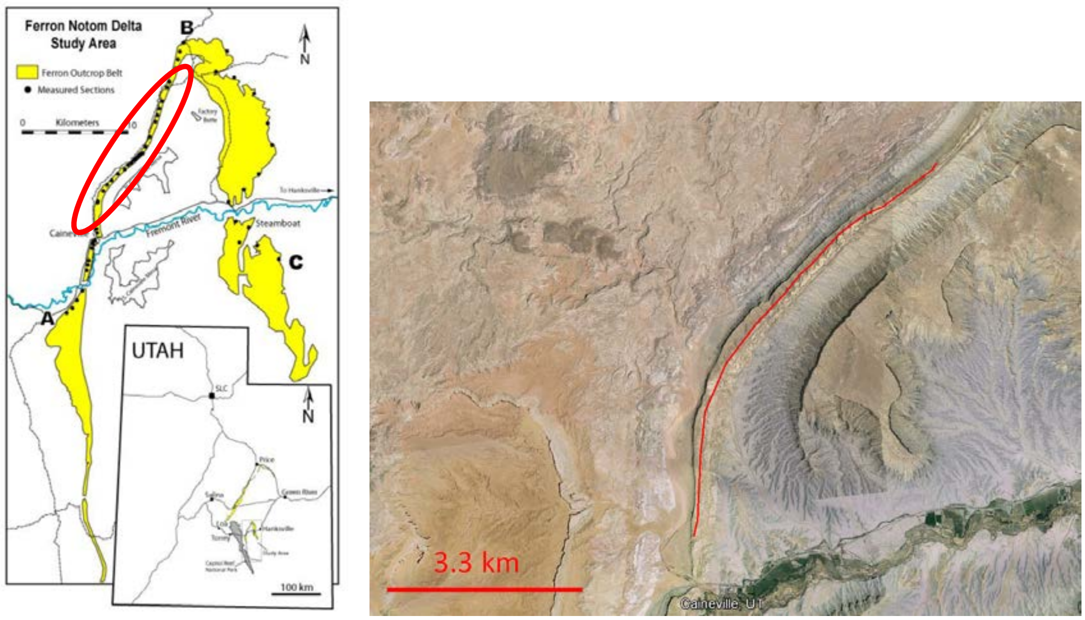

Figure 7A, 7B: On the left, a map of older measured sections used for regional stratigraphy; red ellipse shows area of interest for this study (Zhu, 2010) and on the right, the study area follows the east-dipping ridge outlined in red (Google Earth)

3. Methodology

Eleven measured sections running approximately north-south in a basinward direction provided the primary data set for this study and record grain size and sorting, cross set thickness, sedimentary structures, and the degree of bioturbation and paleocurrent directions. The resulting correlation provides a more detailed dip-oriented view of sequence 2 stratigraphy for comparison with the earlier, regional scale cross section (Zhu et al., 2012). The facies were grouped into the lithofacies previously established by Zhu et al. (2012) and provide a basis for comparison with valley fill facies models (e.g., Boyd, 2006; Zailtin et al., 1994, and others) and enable the documentation of the downstream succession of depositional environments. The results can also be compared with other, younger incised valleys found in sequence 1 of the Ferron (Li et al., 2010). Extensive exposures of SB 1 and 2 enabled these surfaces to be walked out and traced laterally (primarily along dip). Additionally, high resolution photographs enabled the creation of photomosaics, which in turn provided a basis for a bedding diagram.

In conjunction with these data, a variety of informative calculations can be performed. Observing lapout relationships and combining this with the slope estimations and the distribution of facies can reveal backwater length (Paola and Mohrig, 1996; Blum and Törnqvist, 2000; Bhattacharya, 2014). Likewise, the appearance of tidally influenced facies may represent deposition within the bayline (Blum et al., 2013).

Additionally, flow depth calculations were derived from the Leclair and Bridge (2001) method. Assuming one-third preservation of dune thickness in a cross set, and using a scaling factor of 6 to 10 times the cross set thickness, an approximate depth range is established and compared with thicknesses of fully preserved storey, which can also be used as a proxy to estimate bankfull flow depth. Strike-view cross sections can also be used to make width estimates of formative channels, especially where channels are single-thread meandering streams.

From these types of data, water and sediment discharge estimates can be made (Bhattacharya and Tye, 2004; Bhattcharya and MacEachern, 2009; Davidson and North, 2010; Blum et al., 2013; Holbrook and Wanas, 2014).

Results

4.1 Facies Descriptions and Interpretations

The Ferron outcrops described here contain the full range of depositional environments and facies associated with deltas (Li et al., 2010; Zhu, 2012 and others). At the most paleo-landward locations are the fluvial trunk channels. Towards the north, the paleo-seaward direction, the fluvial systems become incised (Li et al., 2010) and then transition to a variety of mixed energy, paralic, estuarine, and nearshore facies, (Garza, 2008; Li, 2012). At the most seaward locations, a variety of shallow marine facies have been documented including delta-front and shoreface deposits of varying fluvial, wave and storm influence, which are temporally equivalent to, and fed by, the sequence 2 fluvial valleys documented here (Li, in press).

The facies scheme of Zhu et al. (2012) is adopted here, minus those facies which are not found in this study area. Nine facies have been grouped into fluvial, estuarine, and marine facies associations. The descriptions and interpretations of these facies are summarized in Table 1.

Facies Association	Facies	Interpretation	Lithology & Sedimentary Structures	Biota
FA1: Fluvial Facies	1	Fluvial channel fill	Erosional base with very coarse to pebble scale lag, mud rip up clasts and wood debris, upper fine to upper medium tabular and trough cross bedding with varying degrees of tidal influence in the form of double mud drapes and local heterolithic and flaser bedding, generally fines up section	Generally absent, BI ≤ 1 at top of channel fill with ichnogenera: *Skolithos* and *Planolites*
	2	Floodplain	Silty mudstones interbedded with coal seams and local very fine to fine grained, rippled sandstone beds, rooting is present	Absent, BI=0
	3	Distributary channels	Erosional base with mud rip up clasts and wood debris, exhibits bar scale, dune scale cross bedding (tabular and trough) composed of fine to medium grain size sandstones	Absent to low, BI=0-2 with ichnogenera: *Planolites* and *Ophiomorpha*
FA2: Estuarine Facies	4	Bayhead delta	Very fine upper to fine grained sandstone beds (≥ 10 cm thick) with hummocky and swaley cross stratification or ripples (current and combined flow), interbedded with mudstones and soft sediment deformation	Variable, BI=0-4 with ichnogenera: *Planolites* and *Thalassinoides*
	5	Lagoonal and bay fill	Very fine lower to fine grained sandstones with hummocky and swaley cross bedding ≤ 1 meter thick, ripple (current and wave) and planar lamination, interbedded with silty mudstones and soft sediment deformation	Low to intense, BI=2-5, with ichnogenera: *Teichicnus* , *Planolites* , *Thalassinoides* , *Chondrites* and *Ophiomorpha*
FA3: Marine Facies	6	Lower shoreface	Very fine to fine hummocky and swaley cross bedding up to several meters thick, with thinner sandstones with planar and wave ripple laminations and scattered mud drapes	Low to complete, BI=1-6 with ichnogenera: *Ophiomorppha, Thalassinoides* , *Asterosoma, Rosselia, Palaeophycos* and *Macaronichnus*
	7	Upper shoreface	Upper fine to lower medium cross bedded (tabular and trough) sandstones with an increase of grain size at basal contact	Absent to low, BI=0-2 with ichnogenera: *Skolithos* and *Ophiomorpha*
	8	Prodelta	Generally massive mud and siltstones with thin (<10cm), very fine grained sandstones with planar transitioning to rippled laminations interpreted as Bouma sequences, soft sediment deformation is common	Absent to low, BI=0-2 with ichnogenera: *Planolites* and *Skolithos*
	9	Shelf mudstones	Shale with rare, thin bedded, very fine grained sandstones with ripples as well as massive silt and mudstones	Low to intense, BI=2-5, with ichnogenera: *Zoophycos* , *Planolites* and *Chondrites*

Table 1: Descriptions and interpretations of observed facies. Facies scheme adapted and modified from Zhu (2012). Bioturbation scale from Taylor and Goldring (1993) after Reineck (1963)

4.1. Facies Association 1: Fluvial Facies

Facies 1 Description

Facies 1 is by far the most prevalent facies and primarily contains white to cream colored, upper fine-to upper medium-grained sandstones underlain by an undulating, erosional base containing coarse to pebbly grains and occasional permineralized woody debris. This base represents a sharp increase in grain size from underlying facies. Although some dune-scale tabular (planar) cross bedding is observed, dune-scale trough cross bedding is the most common sedimentary structure. The average thickness of cross sets is 18.5 centimeters (n=45). The dip direction of cross bedding foresets and occasional plan-view rib and furrow structures enable measurements of paleocurrent directions (Fig. 8). Rare, sporadic ripples are found capping some dune-scale cross bedding. Sandstone bodies can be as thick as 20 meters, although most measured sections encountered no more than 10 vertically continuous meters of Facies 1.

The sandstone bodies are multiple storeys thick and are intermittently exposed along the hogback ridge, but appear to have been laterally continuous from south to north, prior to recent erosion. In many sections, a fining upwards trend is readily apparent, but is occasionally broken by a sharp increase in grain size, mid-section. Fining upward units do not exceed 6 meters in height (Fig. 9). This grain size jump is also associated with mud clasts and woody debris, including logs. This jump is particularly well developed at measured sections 13-5 and 13-6. Additionally, many sections contain varying amounts of mud drapes on the foresets of cross beds and sometimes in pairs

(Fig. 10). The frequency and density of these drapes appear to increase up section. Minimal bioturbation is observed but where present, appears in the form of simple vertical and horizontal centimeter scale burrows (perhaps *Skolithos* and *Planolites*) at the tops of fining upward sections.

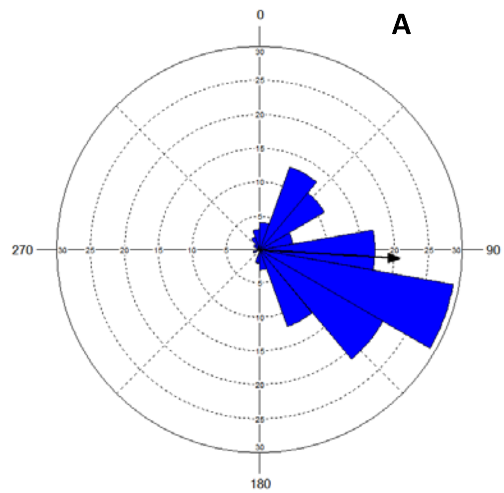

Figure 8A: Rose diagram for all paleocurrent directions measured from dip of foresets and plan-view exposures of rib and furrow structures (n=124, average direction is generally east) (created with Oriana 4 software)

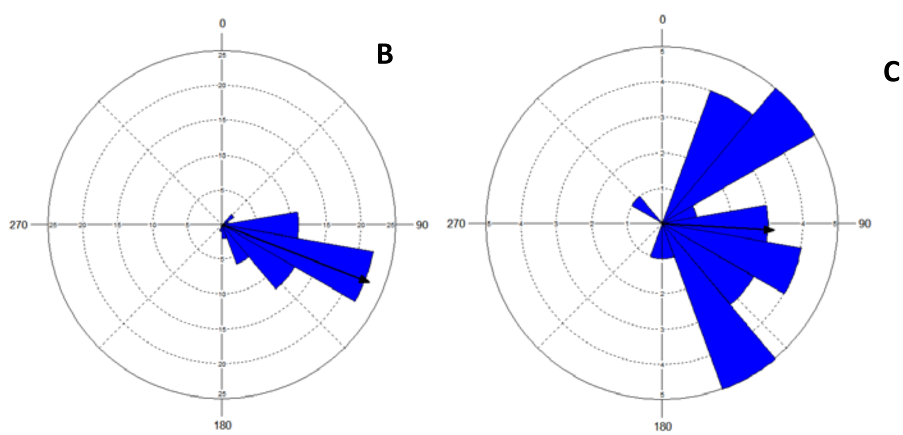

Figure 8B, 8C: Rose diagram for the upper and lower fluvial valleys separately. The upper valley shows consistent measurements towards East-South-East while the lower valley shows considerably more scatter but similar average eastern direction (n=57 and 28 respectively) (created with Oriana 4 software)

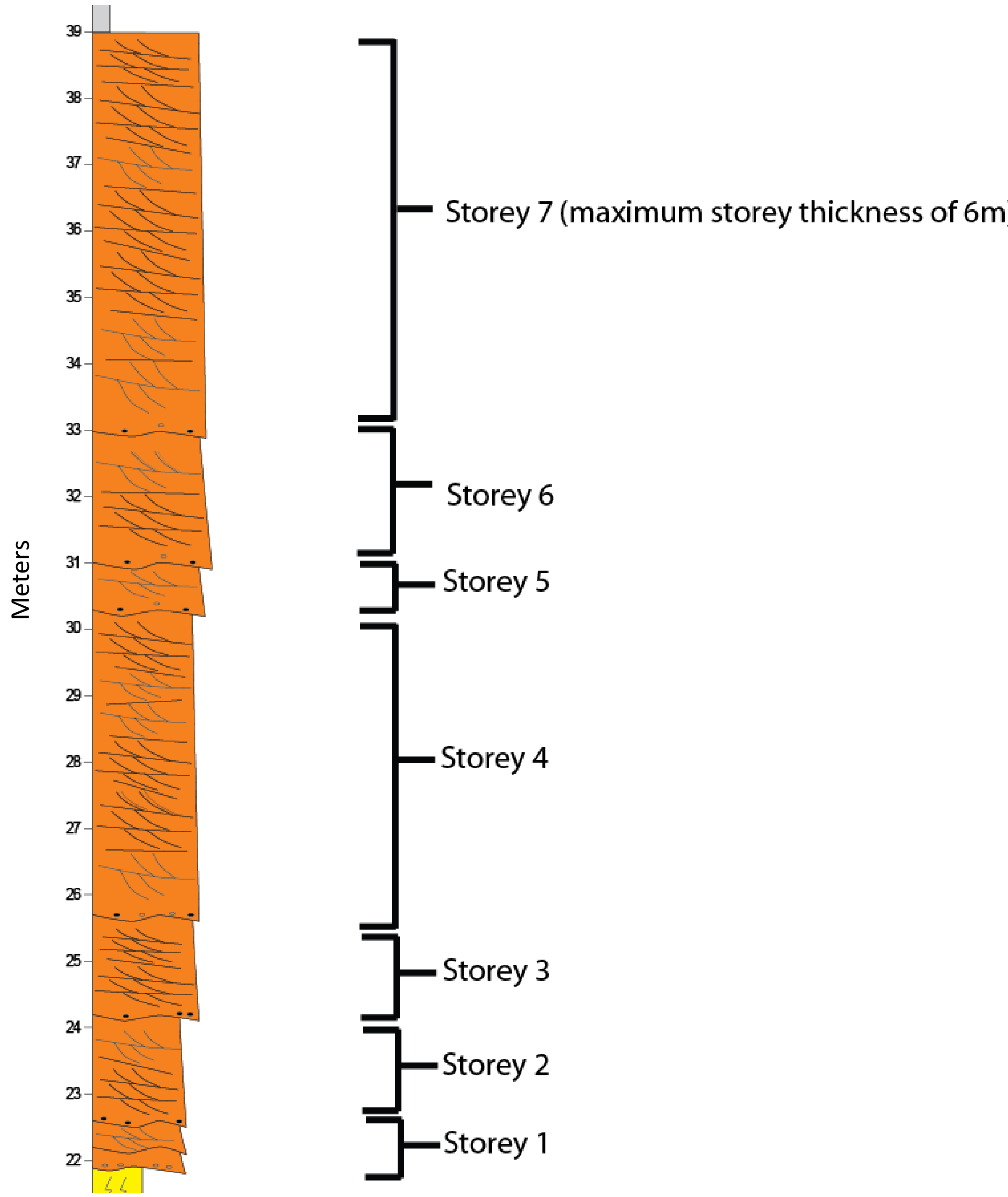

Figure 9: Fluvial portion of sequence 2, from measured section 13-1, showing several amalgamated fining upward units (storeys) which, individually, are no more than 6 meters thick. This observation holds true for fining upward units in all measured sections.

Facies 1 Interpretation

Facies 1 is interpreted as a multi-storey fluvial channel fill with an erosional basal scour and associated pebbly lag. Using the Leclair and Bridge (2000) method, average cross-set thickness of 18.5 cm suggests formation from dunes which stood approximately 55 to 56 cm tall. Assuming flow depth ranges from 6 to 10 times dune height, lower and upper bounds for flow depth of 3 to 5.5 meters, are estimated respectively. Relative to the thickness of the sandstone bodies, these flow depths suggest that the deposits are a multi-storey amalgamated fluvial system, probably confined to an incised valley whose base is defined by the basal erosional surface. This is comparable to the fluvial systems in Sequence 1 (Li et al., 2010).

The fining upward trend is ascribed to waning fluvial transport capacity, although the sharp mid-section grain size increase observed in measured sections 13-5 and 13-6 is interpreted as another erosional surface due to fluvial incision with renewed fluvial deposition associated with a distinct upper valley (Fig. 10A, 10B). In other words, the valley in Sequence 2 is interpreted to have undergone multiple episodes of cut and fill and is therefore compound. Averaged paleocurrent measurements are interpreted as indicative of the direction of fluvial transport and exhibit a generally eastern trend (Fig. 10A) but are also broken down into measurements for each interpreted valley (Fig. 10B, 10C) and, notably, the upper valley does contain a stronger trend with less paleocurrent direction scatter. A slight bidirectional component seen in the lower valley, which is interpreted as indicating tidal influence. Additionally, the mud drapes (Fig. 10C, 10D, 10E, 10F) are interpreted as evidence for low energy slack water conditions, and because they occur in regular pairs, the drapes are interpreted as being the result of diurnal tidal effects. The increased prevalence of mud drapes up-section and towards the north are interpreted as representing increased tidal influence both over time (especially in the upper valley) and towards the north, the paleo-seaward direction.

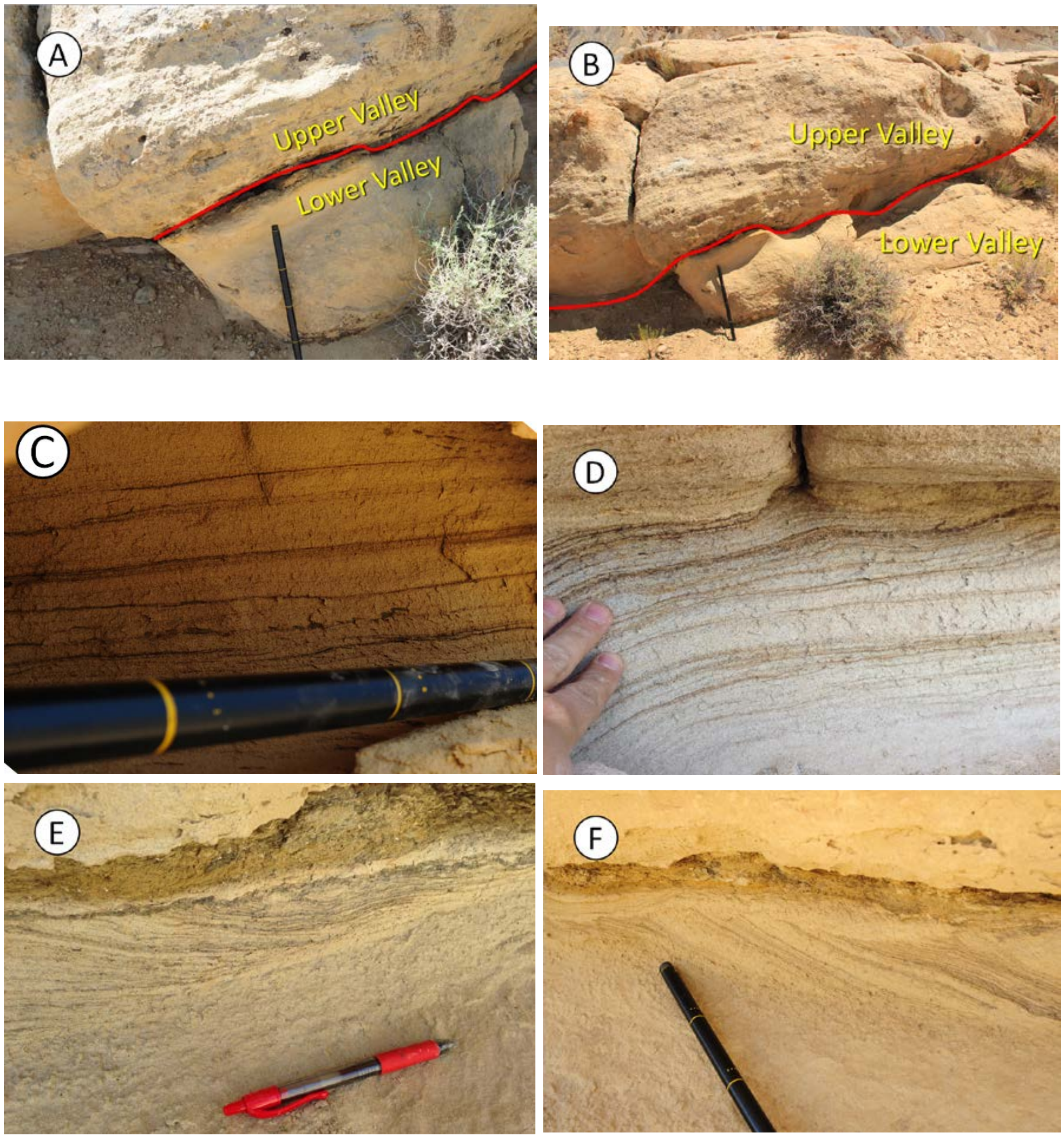

Figure 10: Fluvial facies. A) Inter-valley contact, close-up. B) Inter-valley contact, zoomed out. C) Double mud drapes at section 13-7. D) Double mud drapes and possible Flaser bedding at section 13-1. E) Double mud drapes at section 13-5. F) Double mud drapes at section 13-6.

Facies 2 Description

Facies 2 is comprised primarily of grey to black, meter-scale planar and massive silty mudstones, which are interbedded with carbonaceous material and coal seams. There are sporadic local occurrences of thin (<20 cm) bleached white to cream and rust colored, very fine-to fine-grained sandstone beds, which are exposed to varying degrees and can exhibit asymmetric ripples, planar stratification, or be apparently structureless (massive). Root traces are extensive in conjunction with abundant centimeter-scale slickensides.

Facies 2 Interpretation

Facies 2 is interpreted as floodplain mudstones with rare interbedded sandy crevasse splay deposits. The pedogenic features indicate long-term subaerial exposure, which facilitates rooting, whereas the slickensides are interpreted as evidence of the repeated cycles of wetting and drying expected in floodplain settings. Bleached, rooted sandstones are also seen as evidence of prolonged subaerial exposure. This facies is seen at the interpreted Sequence Boundary 1 in the southernmost measured sections (sections 13-1 through 13-4) and also between sequence 2 fluvial deposits at section 13-4. The lack of floodplain deposits within the fluvial channel fill implies a confined nature of the fluvial system, where conversely, an unconfined fluvial system ought to regularly encounter alternating sandy fluvial channel and muddy overbank fines associated with avulsion and meandering of the channel belt. Another floodplain and interpreted exposure surface (with stratigraphic implications) occur immediately above the upper fluvial channel fill between sections 13-5 and 14-1 (Fig. 11) but are themselves overlain by more distal, estuarine facies before being capped by Sequence Boundary 1 and the renewed fluvial deposition.

Facies 3 Description

Facies 3 features an undulatory, erosional base with muddy clasts and woody debris, similar to that observed in Facies 1. Grain size varies but is generally between very fine upper to fine upper. Sedimentary structures include meter-thick occurrences of 2D and 3D (tabular and trough) dune-scale cross bedding in addition to asymmetric ripples. In some cases, a minor fining upward component is observed. Bioturbation ranges from absent to low (Bioturbation Index of 0-2) and consists of simple, centimeter-scale horizontal burrows and slightly larger curved burrows with rough, poorly defined walls (*Planolites* and *Ophiomorpha* respectively).

Facies 3 Interpretation

Facies 3 is interpreted as deposition associated with distributary channels and their descriptions largely mirror that of Facies 1, but these sandstone bodies are smaller in scale (under 1 meter thick) and isolated in a lateral and vertical sense and lack the distinct extra-formational pebble lag at the base of F1, fluvial channel fill.

4.1. Facies Association 2: Estuarine Facies

Facies 4 Description

Facies 4 is dark grey and brown, heterolithic (Fig. 11), and contains very fine-upper to fine-grained sandstone beds (≥10 cm thick) with long wavelength, meter-scale cross bedding (hummocks and swales), as well as current and combined flow ripples which are interbedded with mudstones that lack signs of subaerial exposure. Soft sediment deformation is fairly extensive (Fig. 11). Trace fossils include simple horizontal *Planolites* burrows, which are observed in conjunction with branching *Thalassinoides* burrows. The degree of bioturbation ranges from none to relatively high (BI of 0 to 4). A weak upward coarsening trend is identified in some sections (13-5, 13-7 and 14-1).

Facies 4 Interpretation

Facies 4 is interpreted to represent a bayhead delta facies. In outcrop, the facies is clearly heterolithic, and the lack of pedogenic features, in combination with some bioturbation, suggests a paralic facies. Facies 4 lies above the compound incised valley, which suggests that estuarine flooding facies filled the formerly fluvial incision. Distinguishing bayhead delta from bay fill is difficult, however, because both facies occur in similar (but not identical) depositional environments. To distinguish bayhead deltas from open marine facies (e.g. prodelta), the relative lack of bioturbation and reduced diversity of ichnogenera caused by brackish depositional environments is a useful identifier.

Estuarine facies are observed in measured sections 13-5 through 14-1, and it follows that they should be found only at more paleo-seaward (northern) locations.

Facies 5 Description

Facies 5 is dark grey and brown, heterolithic (Fig. 11), and contains very fine-lower to fine-grained sandstones, which exhibit long wavelength hummocky and swaley cross stratification, current and wave ripples, and some planar lamination. Sand beds are no more than 1 meter thick, but are more often decimeter scale. Sandstone beds are interbedded with silty mudstones with a greater muddy component than seen in Facies 4. Again, some soft sediment deformation is present. Bioturbation varies, but ranges from low to intense (BI of 2 to 5) and ichnogenera include, but are not limited to, *Teichicnus*, *Planolites*, *Thalassinoides*, *Chondrites*, and *Ophiomorpha*.

Facies 5 Interpretation

Like Facies 4, Facies 5 is a complex paralic facies and it is interpreted as an estuarine central bay fill facies, in proximity to the previous bayhead delta facies. Facies 5 is also clearly heterolithic and lacks subaerial exposure or pedogenic features and also exhibits a relatively high degree of bioturbation, with ichnogenera representing a mixture of *Skolithos* and *Cruziana* ichnofacies. Bay fill facies are distinguished from bayhead delta largely on the basis of the increased muddy component and corresponding lack of thicker (meter scale) sandstone beds in conjunction with the slightly higher degree of bioturbation. Judged on these criteria, bay filling facies seem to make up a greater volumetric component of the transgressive estuarine facies association, compared to the bayhead delta association of Facies 4. Again, distinguishing estuarine facies from open marine facies is aided by the reduced diversity of intensity of bioturbation and the presence of ichnogenera which can be found in brackish conditions, such as *Teichichnus,* but it should be noted that confirmation of this interpretation would require additional detailed lateral mapping of the extent of the facies in order to unequivocally demonstrate the presence of a protected bay. Facies 5 is found from measured section 13-5 at its southern limit and north to section 14-1.

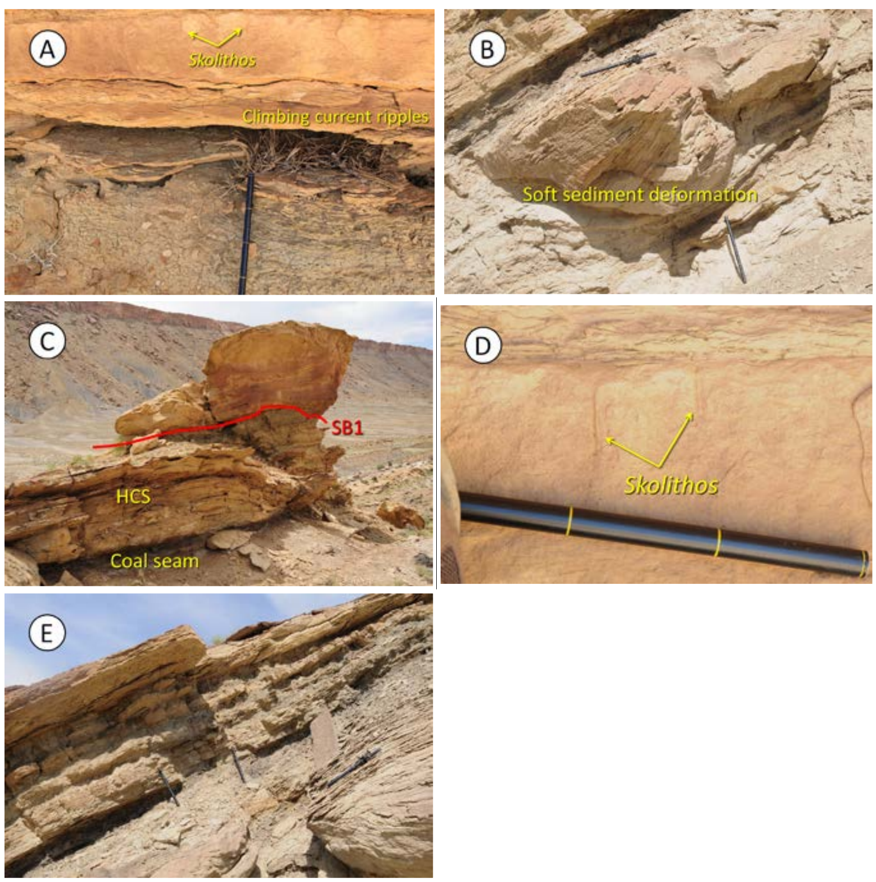

Figure 11: Bayhead delta and bay fill. A) Climbing current ripples above bay fill at section 13-8. B) Soft sediment deformation south of section 13-6. C) HCS and silty bay fill above a coaly, rooted exposure surface and beneath the thick fluvial sands from Sequence 1 at section 13-8. D) Simple vertical *Skolithos* burrows at section 13-8. E) Bay fill south of section 13-6

4.1. Facies Association 3: Marine Facies

Facies 6 Description

Facies 6 contains upper very fine-to lower fine-grained, yellow to beige sandstones with thin decimeter-scale planar and symmetric wave rippled beds (Fig. 12), coarsening upwards into extensive hummocky and swaley cross bedding. Amalgamated HCS sandstones are up to 7 meters thick. Most occurrences of Facies 6 are capped by an undulatory, erosional surface with an abrupt increase in grain size (Facies 1). Sporadic instances of mud clasts and mud drapes are found in some of the thick HCS sandstone beds. Bioturbation varies from low to pervasive (BI of 1 to 6) with a wide variety of ichnogenera, including *Ophiomorpha*, *Thalassinoides*, *Asterosoma*, *Rosselia*, *Palaeophychos,* and *Macaronichnus* (Fig. 12).

Facies 6 is observed stratigraphically beneath the Facies 1 fluvial facies at every measured section location, and is also found between the lower and upper fluvial valleys at section 13-7 (Fig. 12, Fig. 14) and every section north from that point.

Facies 6 Interpretation

Facies 6 is interpreted as a shallow-marine lower shoreface deposit. The upward coarsening, extensive HCS bedding (Fig. 12) and extensive *Cruziana* and *Skolithos* ichnofacies are strong criteria for the lower shoreface interpretation (Clifton, 2006). This shoreface body expands rapidly toward the north and has important stratigraphic implications (see discussion section 5.2).

Facies 7 Description

Facies 7 comprises yellow to beige, upper fine-to lower medium-grained sandstones containing dune-scale tabular and trough cross bedding and with a distinct increase of grain size at its basal contact. Sandstone beds coarsen upwards and are several meters thick. Bioturbation is absent to low (BI index of 0 to 2) with ichnogenera limited to *Skolithos* and *Ophiomorpha*.

Facies 7 only occurs beneath Facies 1 fluvial valleys at the northernmost measured section, section 14-1. At this location, lower shoreface facies 6 coarsens upwards into facies 7.

Facies 7 Interpretation

Facies 7 is interpreted as an upper shoreface facies. The coarser grain size (upper fine minimum) and presence of dune-scale cross bedding, in conjunction with reduced bioturbation versus the underlying lower shoreface, indicate a more proximal location and shallower deposition within fair-weather wave base. Assuming sand grains are supplied by a deltaic system, then the transition from lower shoreface to upper shoreface may reflect progradation of a paleo-shoreline.

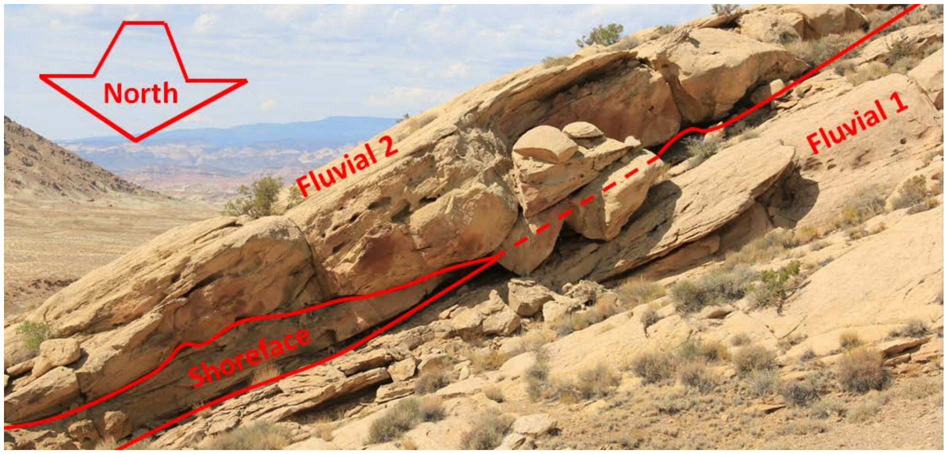

Figure 12: Key outcrop at section 13-7 showing the vertical transition from fluvial to shoreface and back to fluvial facies

Facies 8 Description

Facies 8 is composed of generally massive, dark blue-grey mudstone and siltstones, which are interbedded with sporadic, thin (<10 cm thick), very fine-grained sandstones. Some sandstone beds show planar laminations which transition upwards to ripple laminations. Sporadic soft-sediment deformation is observed, some of which disturbs the orientation of thin sandstone beds. Some bioturbation (BI of 0 to 2) is observed in sandstone beds including *Planolites* and *Skolithos* ichnogenera. Facies 8 generally coarsens upwards, with a steady increase in occurrence of sandstone beds towards the top of Facies 8.

Facies 8 Interpretation

Facies 8 is interpreted as a prodelta facies. The interpretation is based on the abundance of muddy lithologies with no evidence for subaerial exposure, combined with laminated planar and rippled, thin, bioturbated sandstone beds and a generally coarsening upwards pattern (Zhu et al., 2010). Sandstone beds which grade upwards from planar laminations to ripples are interpreted as partial Bouma sequences with T_b and T_c components, resulting from turbidites or other sediment gravity flows.

Facies 9 Description

Facies 9 is composed of dark grey, massive silty mudstones with isolated and very fine-grained ripple-laminated sandstones. Facies 9 is very similar to facies 8 but contains fewer sandstone deposits. Also, bioturbation varies from low to intense with a variety of ichnogenera including *Zoophycos*, *Planolites,* and *Chondrites*. Facies 9 is only observed intermittently in the lower half of measured section 14-2, which is stratigraphically lower than the other measured sections.

Facies 9 Interpretation

Facies 9 is interpreted as a prodelta shale facies,. The presence of massive silt with few sandstone beds is consistent with a low energy, deeper water environment, while the suite of ichnogenera implies a *Zoophycos* ichnofacies. What sandstones are present are attributed to turbidity current processes as reflected by the presence of partial Bouma sequences.

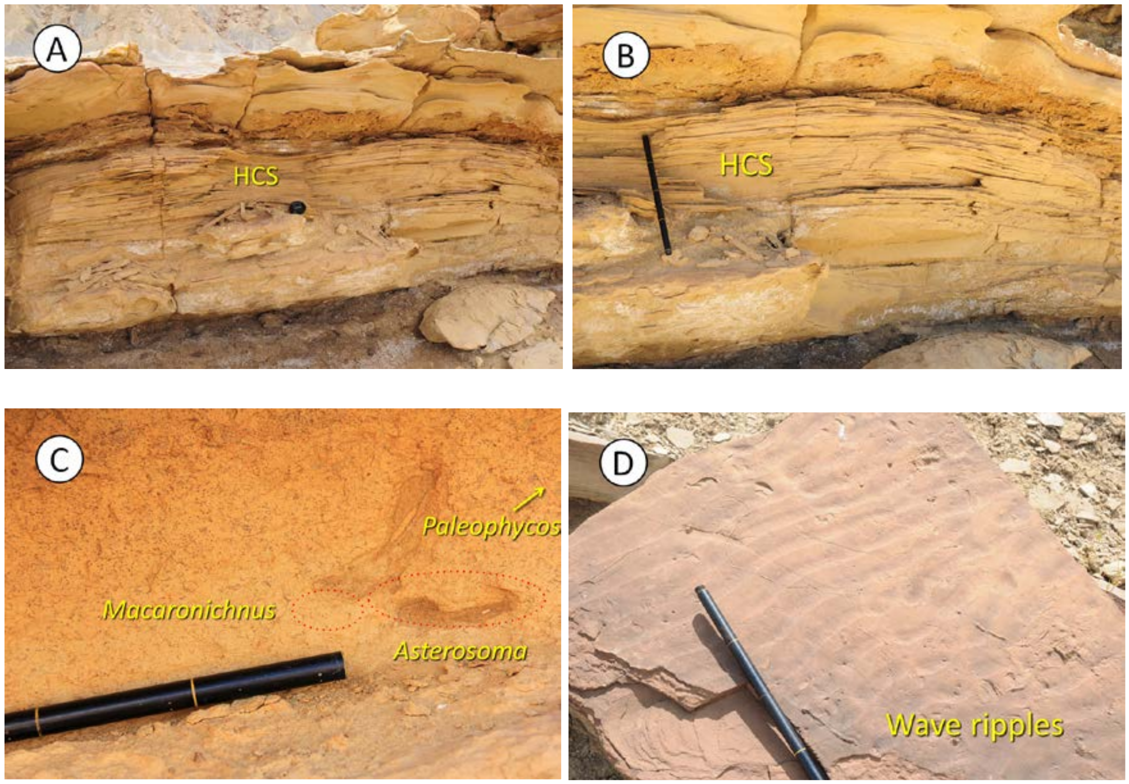

Figure 13: Marine facies. A) HCS in lower shoreface north of section 14-1. B) HCS in lower shoreface north of section 14-1. C) Bioturbation in lower shoreface at section 13-7. D) Thin, symmetric wave rippled very fine grained sandstone in prodelta at section 13-7

4.2. Correlations and Stratigraphy

Most of the data acquired in the field was taken in the form of a series of measured sections along depositional dip, from south to north. In total, 11 measured sections were made (Fig. 14, Fig. 15, Fig. 16) and their naming scheme, derived from Zhu et al. (2012), is by year and by the chronological order of measured sections taken per year (e.g. the second section made in 2013 is section 13-2). 9 measured sections were made in 2013, sections 13-1 through 13-9, and 2 were made in 2014, sections 14-1 and 14-2.

Ten measured sections extend through Sequence 2 and up to Sequence Boundary 1. The underlying parasequence-bounding flooding surfaces were used as stratigraphic datums. This is done because flooding surfaces are assumed to be smoother and flatter than the undulatory and diachronous erosional sequence boundaries (Bhattacharya, 2011), such as Sequence Boundary 2 at the base of the fluvial valleys of interest. The 11th measured section (section 14-2) is used to tie the local flooding surface datum to the regional bentonite datum and to resolve uncertainty regarding the correlation of the parasequence 9 flooding surface in the previously developed regional sequence stratigraphy of Zhu et al. (2012). The first 3 and most southern measured sections, 13-1 through 13-3, are tied to the parasequence 8a on parasequence 8b flooding surface and only penetrate the amalgamated fluvial valleys of sequence 2. All remaining sections are tied to the parasequence 8-parasequence/9 flooding surface, which is locally marked by a pebble lag. This local datum was repeatedly walked out between sections 13-5 and 14-1. Sections 13-5 and 14-1 served as the southern and northern bounds for the local correlation between measured sections (Fig. 17).

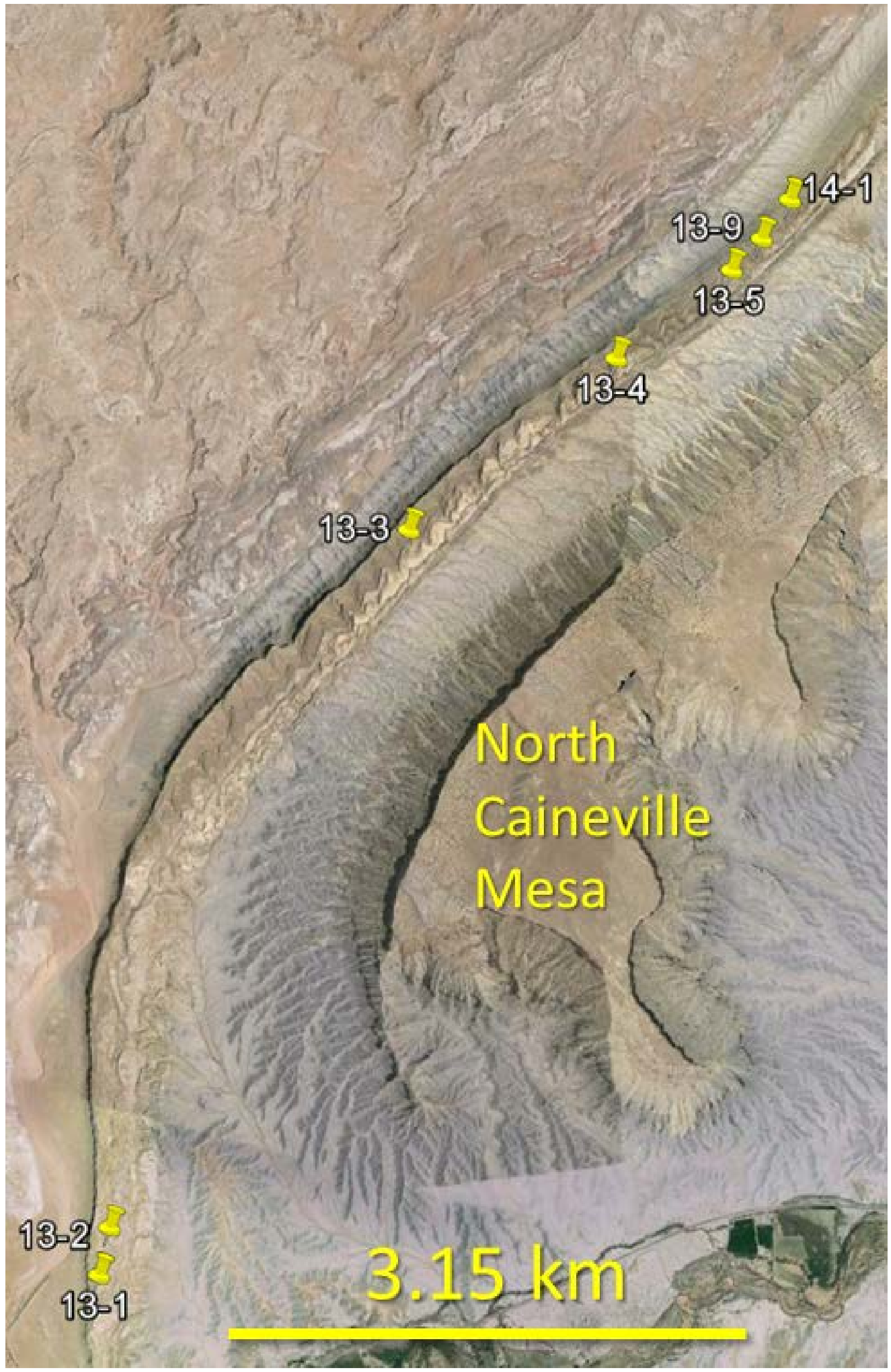

Figure 14: Measured section locations. Note that sections 13-6, 13-7, 13-8 and 14-2 (not shown) have tight ~50m spacing between sections 13-5 and 13-9 (shown). Note also that the wide spacing at southern sections and tight spacing at northern sections is a product of doing detailed work in the northern region in order to decipher stratigraphic relationships
(Image created in Google Earth).

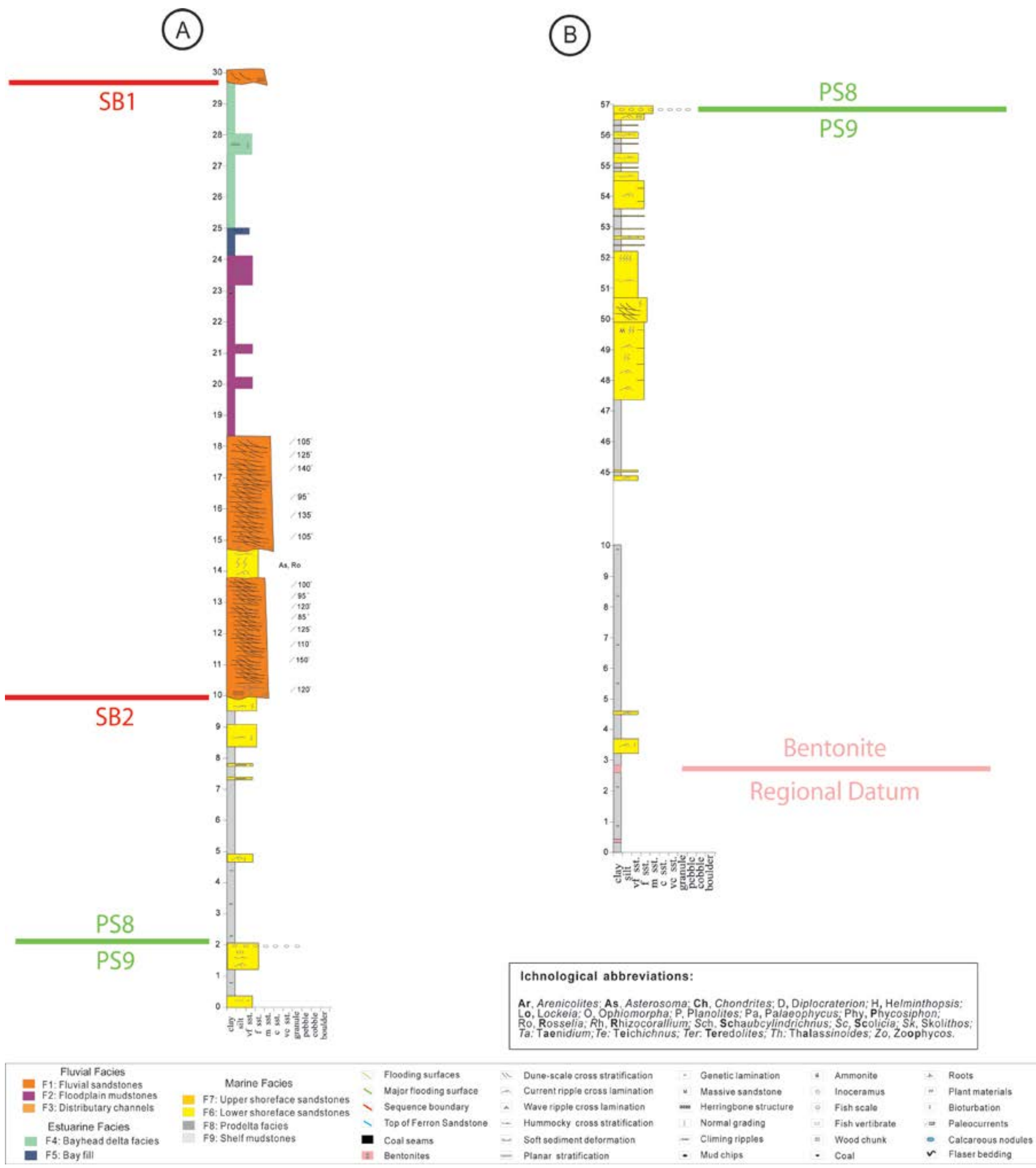

Figure 15: Representative sections. A) Section 13-7 with fluvial-shoreface-fluvial valley fill, topped by floodplain and splays, then estuarine facies and then by SB1. B) Bottom and top of section 14-2 with the regional bentonite datum at the base and the PS 8-9 flooding surface and lag at the top.

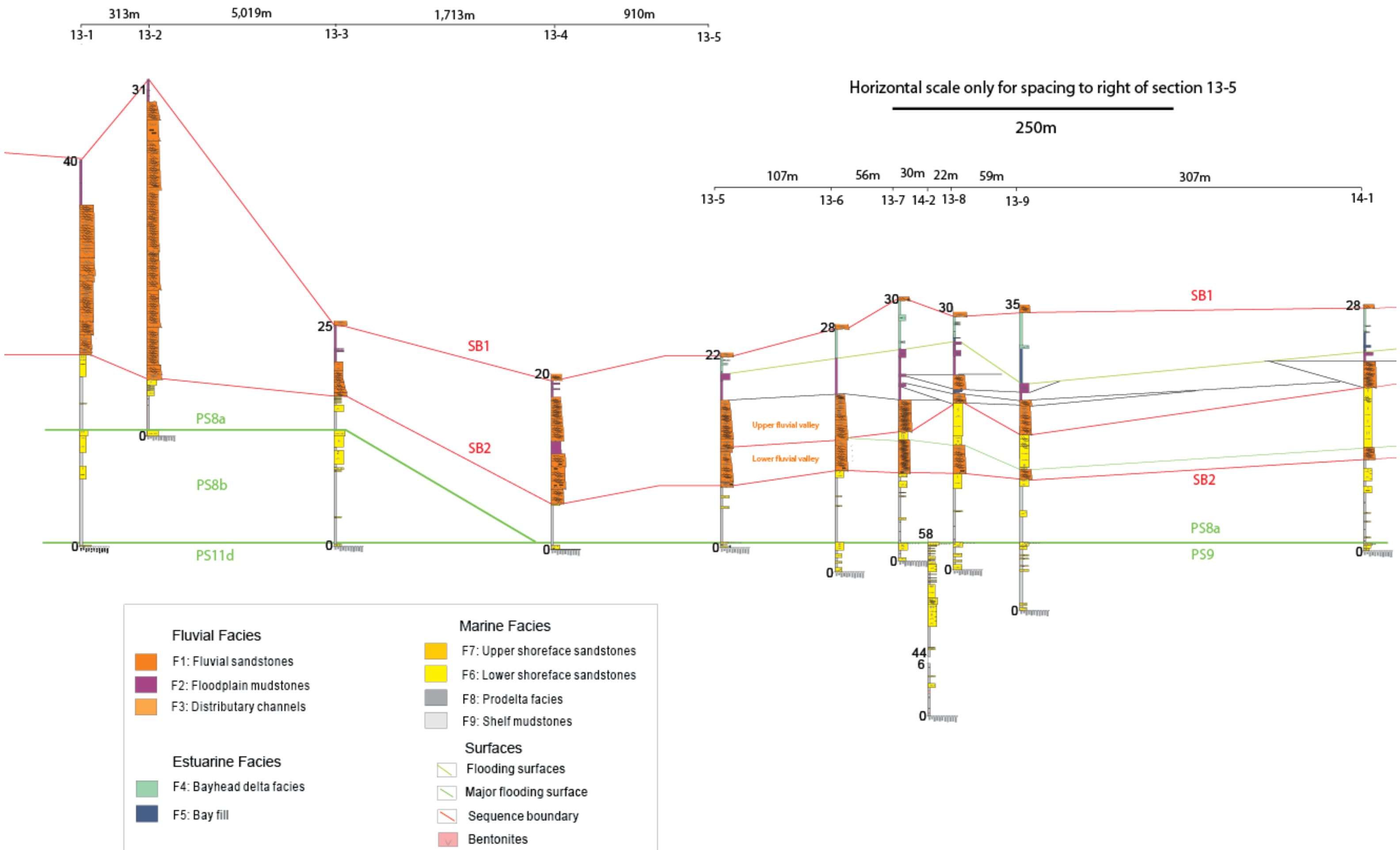

Figure 16: All 11 measured sections with sequence boundaries and datums; relief at SB2 between southern and northern sections is significant. Note that the horizontal scale applies only to spacing right (north) of section 13-5 for display purposes and due to highly variable and very large spacing further south. Also note that section 14-2 is cut between 6 and 44 meters for display purposes. Finally, note that the full legend can be found with the reference measured sections (Fig. 15).

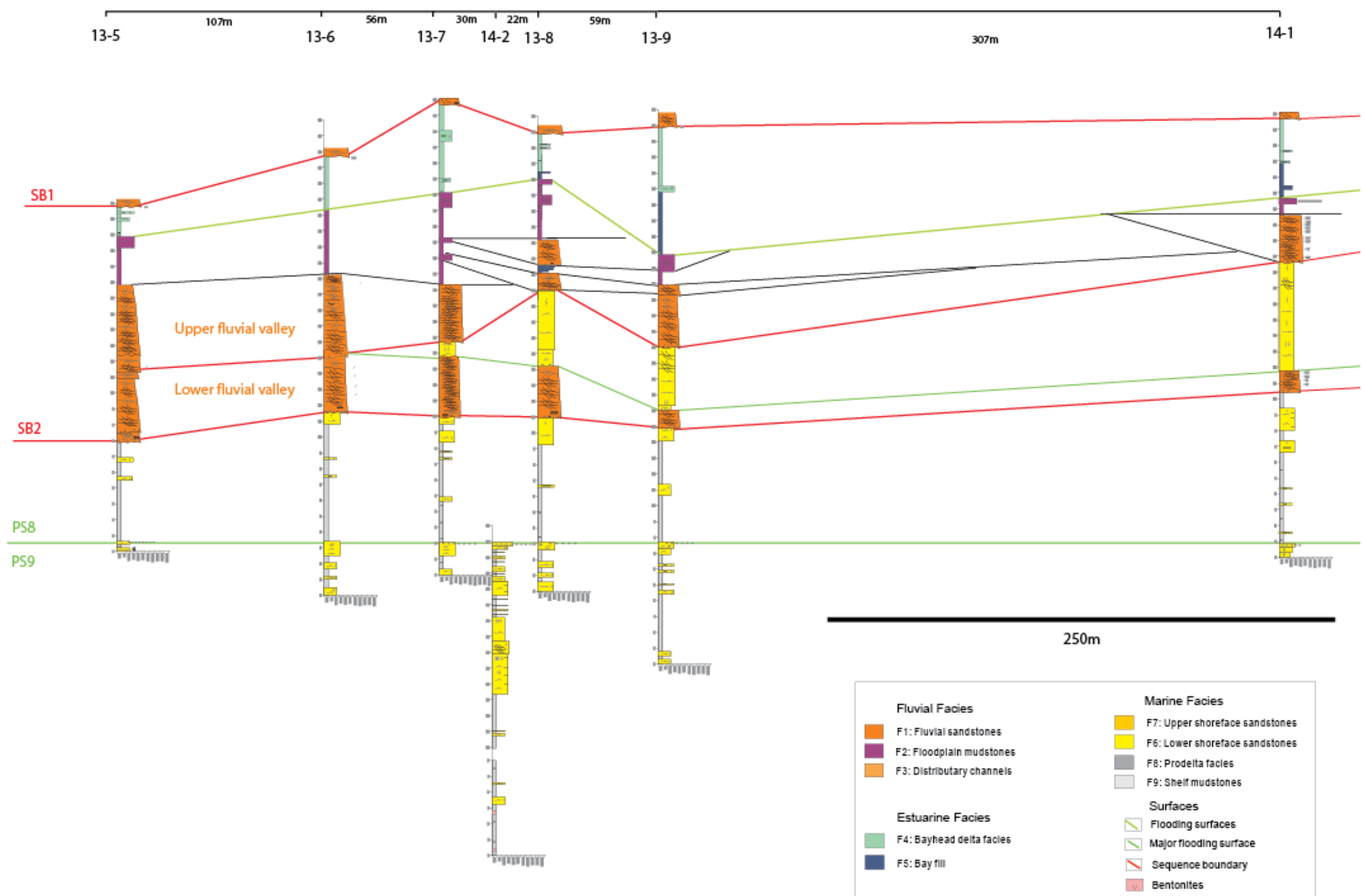

Figure 17: Correlation from sections 13-5 to 14-1. Note that the orange fluvial sands split around the yellow shoreface and demonstrate that the fluvial system underwent multiple episodes of cut-and-fill and is therefore, compound in nature. North is to the right.

4.3 Paleogeographic Reconstruction

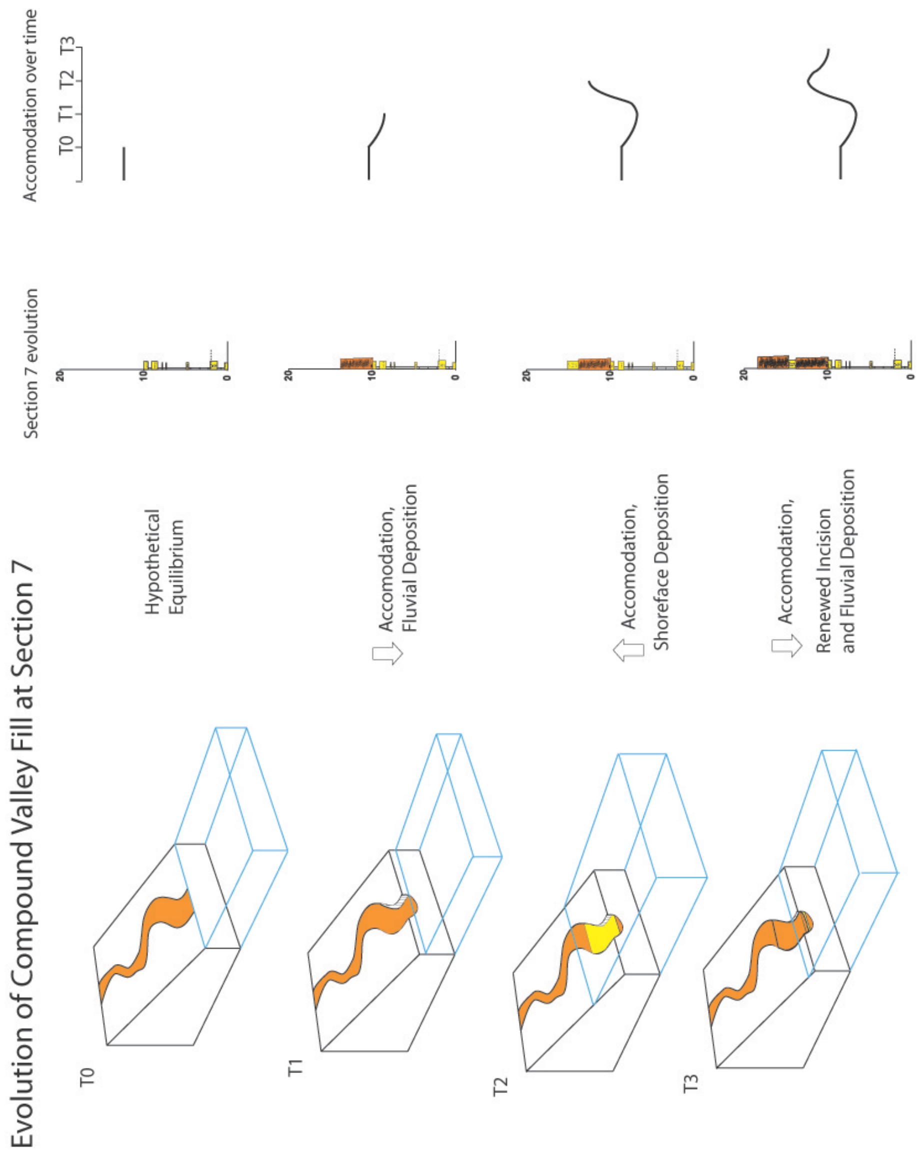

Figure 18: Schematic evolution of deposition of fluvial facies at section 13-7 over time with an emphasis on the interpreted control by variation in accommodation.

5. Discussion

5.1 Applying Traditional Valley Fill Models

Both the Willis (1997) and Zaitlin (1994) valley filling models assume a simple incised valley, but as many recent detailed studies have shown (e.g., Blum et al., 2013), compound incised valleys are common. Li et al. (2010) and Li and Bhattacharya (2013), have already shown that the fluvial valleys in Sequence 1 of the Ferron-Notom delta are compound. Close examination of the older valley system in Sequence 2 has revealed multiple distinct intervals of incision. Additionally, measured section 13-7 and every section north of that location contain a distinct shoreface facies, which interfingers with the fluvial valleys of sequence 2. This vertical sequence is interpreted to be the result of variation in accommodation, and reflects a similar control as invoked to explain the compound nature of Sequence 1 fluvial stratigraphy (Li and Bhattacharya, 2013), as well as the higher-frequency, Milankovitch-scale sequences observed in the regional stratigraphy (Zhu et al., 2012). Here, accommodation is interpreted to have decreased at the start of sequence 2, thus forming Sequence Boundary 2 and resulting in the deposition of the lower fluvial valley. Increased accommodation and subsequent sea-level rise allowed a lower shoreface to transgress the lower fluvial valley. A second drop of sealevel resulted in the second incision of coarser fluvial deposits into this shoreface. Thus we establish Sequence 2 as having at least 2 episodes of cut and fill. Landward, the shoreface deposit onlaps the lower fluvial deposits or is eroded by the incision related to the upper fluvial deposits, thus resulting in an amalgamated fluvial-valley fill.

Above the upper fluvial valley is a rooted exposure surface associated with coal deposits interpreted as floodplain facies and associated crevasse splay deposits (FA2) (Fig. 19) overlain by hummocky cross bedding, burrowed, rippled sandstones, and inter-bedded mudstones lacking roots and coal which indicate subaqueous deposition, assigned to F4, bayhead delta, and F5 bay fill. The exposure surface is indicative of accommodation loss and a possible third loss of accommodation but without renewed fluvial deposition. The overlying estuarine facies indicate a second flooding surface within sequence 2, but not as severe as the first, which brought open-marine lower shoreface over the lower fluvial valley.

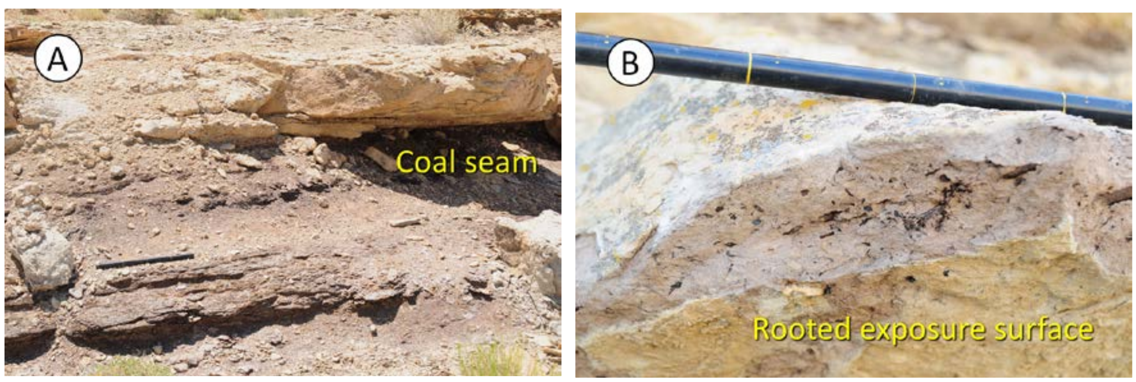

Figure 19: The coal seam and bleached, rooted exposure surface immediately above the upper fluvial valley from section 13-6 to section 14-1

In sequence 2, the lower fluvial valley is capped by lower shoreface deposits, indicating an initially high sediment supply relative to accommodation before accommodation subsequently overwhelms sediment supply, resulting in ravinement and unconformable deposition of lower shoreface units above the fluvial facies. In this scenario, the lower valley would be described as flood capped. The upper fluvial valley lacks associated flooding facies and therefore cannot be described as flood-based or flood-capped according to the Willis model (1997).

Regarding the Zaitlin et al. (1994) segment model (Fig. 1), the lower fluvial valley has segment 1, the proximal fluvial facies, and segment 3, in the form of lower shoreface which fills the valley but lacks estuarine segment 2 facies. If estuarine segment 2 facies were deposited, they were either removed by transgression (ravinement) by overlying segment 3 shoreface or were deposited at other locations, in a lateral direction from deposits measured in sections. Measured sections did not reveal segment 2 estuarine or segment 3 marine facies at coeval intervals with the upper fluvial valley, thus preventing the full application of the Zaitlin et al. (1994) model to the upper valley. Overlying estuarine facies appear to be separated from the fluvial facies temporally (Fig. 19) which agrees with the existing interpretation of regional stratigraphy (Fig. 6) which shows the estuarine facies as coeval with younger paraseqeuence sets 4 and 5.

5.2 Applying the Backwater Concept

Recent models enable the prediction of downstream changes in valley systems. The backwater length concept, as discussed by Blum et al. (2013) and defined by Paola and Mohrig (1996), is particularly applicable with this data set and predicts decreased erosional relief downstream. The interpretation of facies 1 established that the fluvial systems in sequence 2 are in fact valleys and the calculated flow depth of 3.3 to 5.5 meters correlates well with the maximum storey thickness of 6 meters. Relief associated with Sequence Boundary 2 as seen in the regional stratigraphy (Fig. 6) is up to approximately 30 meters in proximal sections. The scale of the erosional relief relative to the established channel depth demonstrates that the sequence 2 fluvial channel fill does qualify as an incised valley system, which should be 5 times deeper than channel depth (Best and Ashworth, 1997) and is particularly evident in measured sections 13-1 through 13-3 (Fig. 16). To the north, the valleys arguably pass basinward into thinner, less amalgamated channels, as the erosional relief correspondingly decreases sharply. Fluvial deposition thins significantly between measured sections 13-3 and 14-1 (Fig. 16).

This decrease of erosional relief is expected in distal, less steep portions of incised valleys and within backwater lengths where amalgamation and avulsion are promoted and floodplain facies onlap more proximal, steep amalgamated, sandy channel belts (Fig. 20) (Paola and Mohrig, 1996; Blum et al., 2013). In the case of sequence 2 fluvial valleys, a slope of .00092 (12 meter drop of erosional base over 13 kilometers in regional cross section) in conjunction with calculated channel depth of 3.3 to 5.5 meters yields a possible range of backwater lengths of 3.6 to 6.0 kilometers. This correlates well with the reduced relief and overlying estuarine facies observed starting at section 13-3 and moving north. The upper fluvial valley pinches out at approximately 1.06 kilometers north of the northernmost section14-1. Thus, the total measured length of the thinner basinward channels and overlying estuarine fill from 13-3 to the northernmost fluvial pinch-out is 4.3 kilometers and falls within the predicted backwater length range. It should be noted that the actual backwater length may be slightly longer because a large gap exists between sections 13-2 and 13-3 (5 kilometers) where the fluvial valleys may thin into channels at a slightly more southern location than 13-3; additionally, recent erosion at the northernmost fluvial pinch-out location may artificially force the fluvial pinch-out at a more southern location than would have been observed in original deposition. Additionally, Blum et al. (2013) correlate slope of the system with shelf transit distance, wherein a slope of ~.001 results in an approximate shelf transit distance of 10 kilometers.

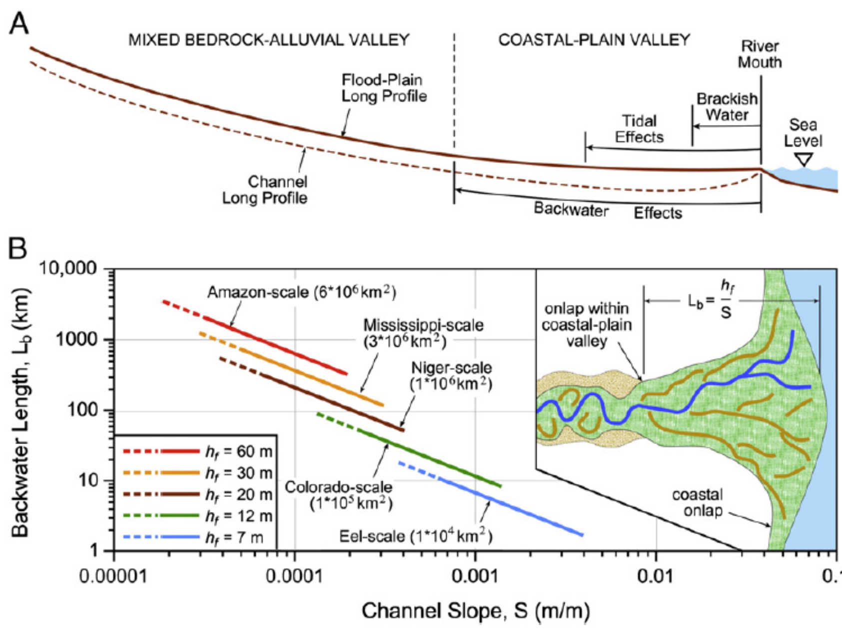

Figure 20: A: Backwater length in a fluvial profile. B: Backwater length as a function of channel slope and flow depth. (Figure from Blum et al., 2013)

5.3 Choice of Datum and Implications for Sequence Stratigraphy

When fitting new measured sections from this work in the stratigraphic area of interest into the regional stratigraphy by Zhu et al. (2012), a variety of facies and surface discrepancies arise. The new measured sections from this work are hung on the local flooding surface that caps parasequence set 9. However, this causes significant differences in the stratigraphic placement of sequence boundary 1 (Fig. 21) compared to the original stratigraphic interpretation (Zhu et al., 2012), which places sequence boundary 1 several meters lower than new sections would indicate. This discrepancy is particularly evident at measured sections 13-7, 13-8, 13-9, and 14-1 (Fig. 21).

To resolve this discrepancy, section 14-2 was measured up from the regional bentonite datum to the local flooding surface datum. This shows a difference from the original correlation of the flooding surface of Zhu et al. (2012). Their correlation shows the surface to be about 5 meters higher than in the newly measured section 14-2. The original interpretation was reasonable, given the widely spaced original sections, but the new, tightly spaced sections, in conjunction with previous sections, suggest a revised correlation in which the top of Parasequence 9 dips towards the north, rather than being relatively flat. Hanging the new measured sections on this re-correlated P9 flooding surface datum greatly reduces the discrepancies in facies observed and in the stratigraphic location of Sequence Boundary 1 (Fig. 22). More specifically, when measured sections 13-7, 13-8, 13-9, and 14-1 are hung on the original correlation of the P9 flooding surface, they show muddy estuarine facies (F4 and F5), whereas older sections 7-37PRE and 7-03 show thick, sandy fluvial deposits. This major difference in observations is resolved when sections 13-7, 13-8, 13-9, and 14-1 are re-hung on the newly correlated, lower flooding surface.

To test the newly interpreted flooding surface correlation, the PSS9 flooding surface was walked out to determine whether it eventually merged with the overlying sequence boundary (SB2) as shown in the regional stratigraphy. New measurements between the PSS9 flooding surface and sequence boundary found a 5.5 to 7 meter separation between the surfaces at 100 meters south of older section 6-05. The previous correlation of the PSS9 flooding surface of Zhu et al. (2012) shows the PSS9 and SB2 surfaces as being merged, rather than separate at this location.

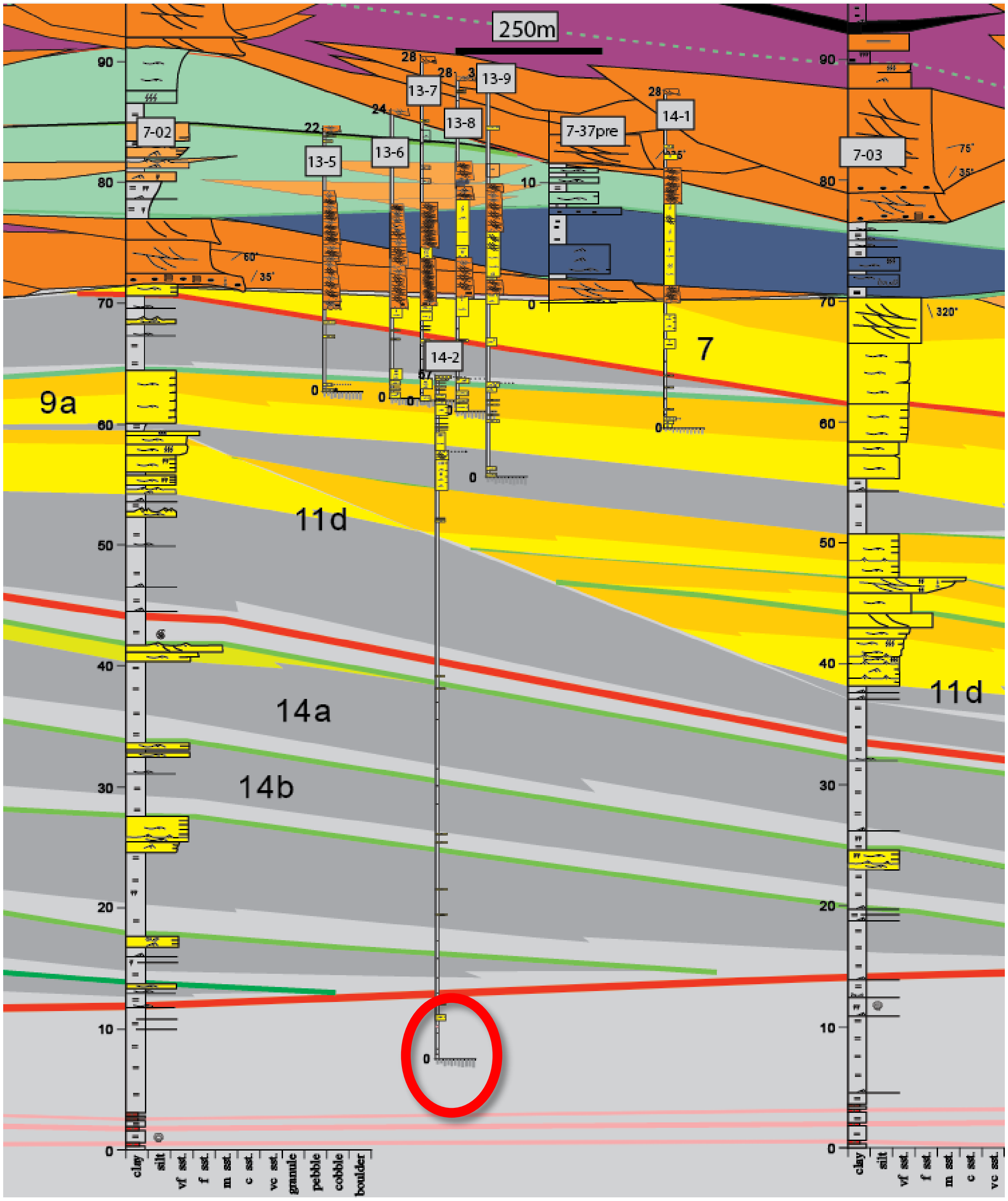

Figure 21: Attempts to tie the new sections' local flooding surface datum to the regional bentonite, while honoring the original flooding surface correlation, failed. Note that bentonite at base of sections 14-2 (red ellipse) fails to reach regional bentonite by at least 5 meters. The only way to honor the regional bentonite was to recorrelate the parasequence 9 flooding surface using section 14-2 to tie the new, lower PSS9 flooding surface to the regional bentonite (Fig. 22). Color code is unchanged from Figure 6.

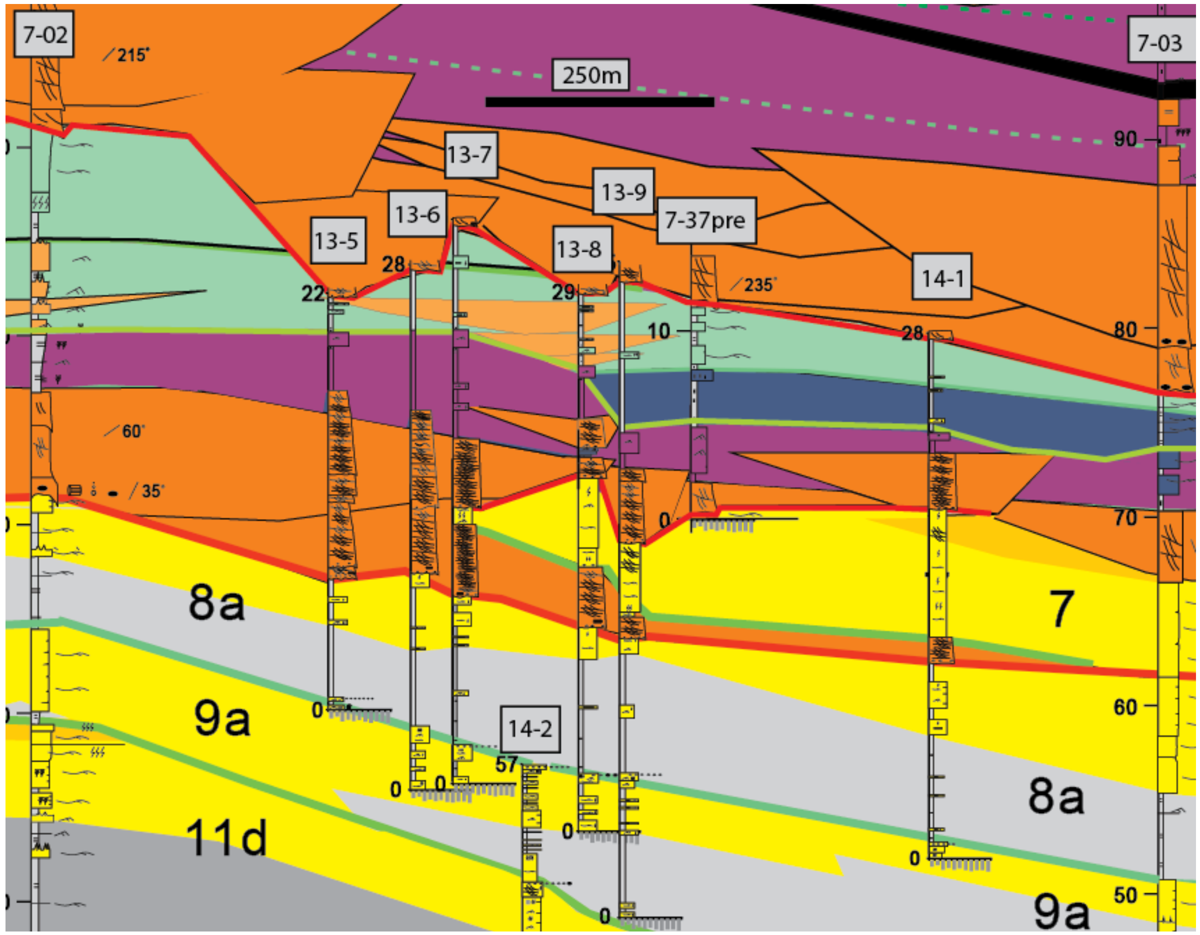

Figure 22: Sections 13-5 through 14-1 are shown, tied to newly dipping flooding surface and shown with original sections 7-02, 7-37pre and 7-03. Preliminary reinterpretation of local stratigraphy is shown. Note that parasequence 9 now drops with its overlying, dipping flooding surface.

5.4 Future Work

Future work on Sequence 2 could include mapping out the northern limits of the upper valley in greater detail which pinches out 1 kilometer north of section 14-1. Beyond that point, any documentation of coeval estuarine or shoreface facies associated with the upper valley would enable the full application of the Zaitlin et al. (1994) valley fill model to the upper valley. Also, mapping out the erosional boundaries of the upper and lower valleys in strike view at Caineville could clarify the exact number of cut and fill episodes and their relative spatial relationships, much as was done for sequence 1 (Li et al., 2010). Also, the exact interplay between the estuarine flooding facies and the floodplains associated with Sequence Boundary 1 can be measured in greater detail between the widely spaced southern sections in this study.

The standing interpretation of the stratigraphic age of the estuarine facies beneath sequence boundary 1 as belonging to parasequences 4 and 5 could also be verified. This would require study of the PSS6 flooding surface at more distal, northern locations. If the regional stratigraphic interpretation of the estuarine facies was incorrect and the estuarine facies were simply the distal expression of parasequences 6 and 7, rather than sharply onlapping the fluvial facies, then the regional stratigraphy would have to be updated to show shazam lines separating the estuarine facies from the more proximal fluvial facies.

This would enable the full application of the Zaitlin model because the estuarine facies would qualify as segment 2 in relation to the incised valley system of parasequence 6. Likewise, this interpretation of the estuarine facies would make the upper fluvial valley flood-topped by the application of the Willis (1997) model.

6. Conclusions

The findings of this work have local and general implications. Locally, the PS9 flooding surface was found to be miscorrelated. The sequence 2 valley system was found to be compound, and the work of Zhu et al. (2012), which emphasized the stepped forced regressive nature of the Ferron-Notom's fluvial systems, is fundamentally sound. In a broader context, the Willis model (1997) and backwater concept (Paola and Mohrig, 1996; Blum et al., 2013) were applicable and demonstrated predictive power, whereas the Zaitlin model (1994) was not applicable given the data available.

Regarding the local implications, it was hypothesized that fluvial valleys in other sequences might also exhibit a compound nature, as documented in Sequence 1. The presence of a shoreface between distinct upper and lower fluvial valleys within Sequence 2 demonstrates that Sequence 2 experienced at least 2 episodes of cut and fill and that, by definition, the fluvial valley in Sequence 2 is also compound. Study of Sequence 1 valley fill invoked accommodation, and specifically, allocyclic eustasy as a control for the valley fill. It was also noted that because each sequence occurred on approximately a 100,000 year time scale, 2 to 4 subdivisions per sequence would imply cyclicity on the order of 25 to 50 thousand years, which approximates the cyclicity of high-frequency Milankovich cycles. The detailed documentation of Sequence 2 fills gaps in the regional stratigraphic data and has shown a miscorrelation of the flooding surface that caps PSS9, requiring the regional stratigraphy to be adjusted, but leaves intact the fundamental conclusions of Zhu et al. (2012) regarding the stepped, forced regressive nature of the Ferron-Notom stratigraphy.

This study showed that the lower valley was flood-topped, and if the overlying estuarine facies were shown to be coeval with the upper fluvial valley, it too would be considered flood-topped. Thus, older valley-fill models, such as Willis (1997), are applicable to the filling of incised valleys, provided that the models are applied in a way that reflects the compound nature of many incised valleys or reflects the non-linear variation in accommodation one would expect, even with a single episode of cut and fill experienced by a simple incised valley. The Willis (1997) model varies accommodation on one level of cyclicity, for simplicity, with accommodation loss or increases happening in a single, linear change. That aspect of the model is unrealistic and the Ferron valleys documented here and by Zhu et al. (2012) demonstrate actual valley fills in the rock record which record intermittent changes in accommodation. The Willis model (1997) is not incorrect when one assumes simple changes in accommodation, but it is important to emphasize the degree to which this major assumption simplifies the model’s valley fills versus the actual rock record.

The Zaitlin et al. (1994) segment model can be applied to the lower valley because the seaward limits of the fluvial facies were found. In this case, the middle segment is missing, possibly as a result of ravinement by the outer segment's shoreface transgression. This suggests the model doesn't take into account the partial preservation experienced in the rock record, in which not all contemporaneous depositional environments will be readily observed.

The upper fluvial valley's paleo-seaward limit was found at a location north of section 14-1, but no additional measured sections were taken there, which would enable the application of the Zaitlin et al. (1994) model for the upper valley. Looking to Zhu et al. (2012) sections at this sequence 2 stratigraphic interval (parasequences 6 and 7), the shoreface at section 7-39 and beyond probably constitute Zaitlin's segment 3 marine facies, but again, the segment 2 facies are missing and partial preservation of depositional environments negates the assumptions that all facies and their relative degrees of marine and fluvial influence will be evident.

The backwater concept (Paola and Mohrig, 1996; Blum et al., 2013) was also shown here to be highly applicable and a powerful tool for predicting downstream changes in valley systems, provided that one can arrive at appropriate estimates of slope and channel depth. The change in slope observed in the distal, low elevation portions of fluvial systems occurs within a few kilometers of coeval shoreline facies, suggesting a short backwater length, consistent with a relatively steep-gradient system. Loss of erosional relief, a more aggradational stacking pattern and deposition of overlying estuarine facies are also consistent with deposition lf the distal valley-pinchout within the backwater. The backwater concept thus has utility in predicting facies and stacking patterns in valley fills in ancient sedimentary systems.

Case studies which test the applicability of models demonstrate the variables which should be considered when making predictions and provide an example of what the actual rocks may look like in relation to models of valley fill end members. Predictions or interpretations of large-scale valley fills which invoke simple, linear changes in accommodation should be treated with skepticism. In other words, compound valleys may be the rule rather than the exception. Additionally, unequal preservation of facies is not uncommon and a mobile shoreline can remove or destroy facies associated with assumed depositional environments, which renders models like the Zaitlin et al. model (1994) more useful as an understanding of potential paleogeographies rather than a tool for predicting preserved facies.

REFERENCES

Armstrong, R. L., 1968, Sevier orogenic belt in Nevada and Utah: Geological Society of America Bulletin, v. 79, p. 429-458.

Best, J.L., Ashworth, P.J., 1997. Scour in large braided rivers and the recognition of sequence stratigraphic boundaries. Nature v. 387, p. 275–277.

Bhattacharya, J.P., and Tye, R.S., 2004, Searching for modern Ferron analogs and application to subsurface interpretation, Chidsey, T.C., Jr, Adams, R.D., and Morris, T.H., eds., Regional to Wellbore Analog for Fluvial–Deltaic Reservoir Modeling, The Ferron Sandstone of Utah: American Association of Petroleum Geologists, Studies in Geology v. 50, p. 39–57.

Bhattacharya, J.P., and MacEachern, J.A., 2009, Hyperpycnal rivers and prodeltaic shelves in the Cretaceous Seaway of North America: Journal of Sedimentary Research, v. 79, p. 184–209.

Bhattacharya, J.P., 2011. Sequence stratigraphy of fluvial–deltaic wedges: a 20 year perspective from the Cretaceous Interior Seaway of North America. Sedimentology 58, 120–169.

Bhattacharya, J.P. and Holbrook, J.M., 2012, Reappraisal of the sequence boundary in time and space: Case and considerations for an SU (subaerial unconformity) that is not a sediment bypass surface, a time barrier, or an unconformity. Earth-Science Reviews v.113, p. 271-302.

Bhattacharya, J.P., 2013, Ancient Backwaters and Baylines: Slope Magnitude and its Control on Deltaic Facies Partitioning in Ancient Deltaic Systems, AAPG Search and Discovery Article #90163, AAPG 2013 Annual Convention and Exhibition, Pittsburgh, Pennsylvania, May 19-22, 2013.

Blum, M.D., and Törnqvist, T.E., 2000, Fluvial responses to climate and sea-level change: a review and a look forward: Sedimentology, v. 47, p. 2–48.

Blum, M.D., Martin, J., Milliken, K., and Garvin, M., 2013, Paleovalley systems: Insights from Quaternary analogs and experiments. Earth-Science Reviews, v. 116, p. 128-169.

Boyd, R., Dalrymple, R.W., and Zaitlin, B.A., 2006, Estuarine and incised valley facies models, Walker, R.G., and Posamentier, H., eds., Facies Models Revisited, SEPM, Special Publication v. 84, p. 171–235.

Bridge, J.S., 2006, Fluvial facies models: Recent developments Facies Models Revisited. SEPM Special Publication No. 84, p. 83-168.

Clifton, H.E., 2006, A re-examination of facies models for clastic shorelines, Facies Models Revisited. SEPM Special Publication No. 84, p. 293-337.

Dalrymple, R.W., Zaitlin, B.A. and Boyd, R., 1992, Estuarine facies models: conceptual basis and stratigraphic implications: Journal of Sedimentary Petrology, v. 62, p. 1130-1146.

Dalrymple, R.W., Boyd, R., and Zaitlin, B.A., 1994, Incised-Valley Systems: Origin and Sedimentary Sequences: SEPM, Special Publication v. 51, p. 381.

Davies, R., Howell, J., Boyd, R., Flint, S., and Diessel, C., 2004, High-resolution sequence-stratigraphic correlation between shallow-marine and terrestrial strata: Examples from the Sunnyside Member of the Cretaceous Blackhawk Formation, Book Cliffs, eastern Utah: American Association of Petroleum Geologists Bulletin, v. 90, p. 1121-1140.

Fielding, C.R., 2007. Sedimentology and stratigraphy of large river deposits: recognition in the ancient record, and distinction from 'incised valley fills. Gupta, A. ed., Large Rivers: Geomorphology and Management. John Wiley & Sons, Ltd, Chichester, p. 97–114.

Gardner, M.H., 1995, Tectonic and eustatic controls on the stratal architecture of mid- Cretaceous stratigraphic sequences, central western interior foreland basin of North America, in Dorobek S.L and Ross, G.M., eds., Stratigraphic Evolution of Foreland Basins: SEPM, Special Publication 52, p. 243–281.

Galloway, W.E., 1989. Genetic stratigraphic sequences in basin analysis I: architecture and genesis of flooding-surface bounded depositional units. American Association of Petroleum Geologists Bulletin v. 73, p. 125–142.

Garza, D., Bhattacharya, J.P., and Zhu, Y., 2008, 3-D facies architecture of a fluvial dominated deltaic system in the Cretaceous Ferron Notom Delta complex: Geological Society of America Abstracts with Programs, v. 40, n. 6, p. 317.

Holbrook, J., & Wanas, H., 2014, A Fulcrum Approach To Assessing Source-To-Sink Mass Balance Using Channel Paleohydrologic Parameters Derivable From Common Fluvial Data Sets With An Example From the Cretaceous of Egypt. Journal of Sedimentary Research, v. 84(5), p. 349-372.

Korus, J., Kvale, E., Eriksson, K., Joeckel, R. 2008. Compound paleovalley fills in the Lower Pennsylvanian New River Formation, West Virginia, USA. Sedimentary Geology v. 208, p. 15-26.

Leclair, S.F. and Bridge, J.S., 2001, Quantitative interpretation of sedimentary structures formed by river dunes: Journal of Sedimentary Research, v. 71, p. 713-716.

Li, W., 2009, Valleys, facies, and sequence stratigraphy of the Ferron Notom delta, Capital Reef, Utah [Unpublished Ph.D. dissertation]: University of Houston, Houston, Texas, p. 139.

Li, W., Bhattacharya, J.P. and Campbell, C., 2010. Temporal evolution of fluvial style in a compound incised-valley fill, Ferron "Notom Delta", Henry Mountains Region, Utah (USA). Journal of Sedimentary Research v. 80, p. 529–549.

Li, W., Bhattacharya, J.P. and Yije, Z., 2011, Architecture of a forced regressive systems tract in the Turonian Ferron 'Notom Delta', southern Utah, U.S.A., Marine and Petroleum Geology, v. 28, p. 1517-1529.

Li, Y., Bhattacharya, J.P., 2013. Facies architectural study of a stepped, forced regressive compound incised valley system in the Ferron Notom Delta, Southern Utah. Journal of Sedimentary Research, v. 83, p.206-225.

Li, Y. and Bhattacharya, J.P., 2013, Falling stage compound valley systems, Ferron Notom Delta. Journal of Sedimentary Research. v. 83, p. 206-225.

Miall, A.D., 1988, Reservoir heterogeneities in fluvial sandstone: lessons from outcrop studies, American Association of Petroleum Geologists, Bulletin, v. 72, p. 682–687.

Miall, A.D., 1994, Reconstructing fluvial macroform architecture from two dimensional outcrops: examples from the Castlegate Sandstone, Book Cliffs, Utah: Journal of Sedimentary Research, v. 64, p. 146–158.

Miall, A.D., 1996, The Geology of Fluvial Deposits; Sedimentary Facies, Basin Analysis, and Petroleum Geology: Springer-Verlag: Berlin, p. 582.

North, C.P. and Davidson, S.K., Unconfined alluvial flow processes: Recognition and interpretation of their deposits, and the significance for palaeogeographic reconstruction: Earth-Science Reviews, v. 111, p. 199-223.

Paola, C., Mohrig, D., 1996. Palaeohydraulics revisited: palaeoslope estimation in coarse-grained braided rivers. Basin Research 8, 243–254.

Posamentier, H.W., 2001. Lowstand alluvial bypass systems: incised vs. unincised. American Association of Petroleum Geologists Bulletin v. 85/10, p. 1771-1793.

Reineck, H.E., and Wunderlich, F., 1968. Classification and origin of flaser and lenticular bedding. Sedimentology, v.11 (1-2), p. 99–104.

Ryer, T.A., 1981, Deltaic coals of Ferron Sandstone Member of the Mancos Shale: Predictive model for Cretaceous coal-bearing strata of Western Interior, American Association of Petroleum Geologists, Bulletin, v. 65, p. 2323-2348

Ryer, T.A., and Anderson, P.B., 2004, Facies of the Ferron Sandstone, east-central Utah, in Chidsey, T.C., Adams, R.D., and Morris, T.H., eds., Regional to Wellbore Analog for Fluvial–Deltaic Reservoir Modeling, The Ferron of Utah: American Association of Petroleum Geologists, Studies in Geology v. 50, p. 59–78.

Shanley, K.W., and McCabe, P.J., 1994, Perspectives on the sequence stratigraphy of continental strata: American Association of Petroleum Geologists, Bulletin, v. 78, p. 544–568.

Van Wagoner, J.C., Mitchum, R.M., Campion, K.M., and Rahmanian, V.D., 1990, Siliciclastic Sequence Stratigraphy in Well-Logs, Cores, and Outcrop: American Association of Petroleum Geologists, Methods in Exploration Series 7, p. 55.

Van Wagoner, J.C., 1995, Overview of sequence stratigraphy of foreland basin deposits: terminology, summary of papers, and glossary of sequence stratigraphy, in Van Wagoner, J.C., and Bertram, G.T., eds., Sequence Stratigraphy of Foreland Basin Deposits, Outcrop and Subsurface Examples from the Cretaceous of North America: American Association of Petroleum Geologists, Memoir 64, p. ix–xxi.

Van Wagoner, J.C., 1995, Sequence stratigraphy and marine to nonmarine facies architecture of foreland basin strata, Book Cliffs, Utah, USA, in Van Wagoner, J.C., and Bertram, G.T., eds., Sequence Stratigraphy of Foreland Basin Deposits, Outcrop and Subsurface Examples from the Cretaceous of North America: American Association of Petroleum Geologists, Memoir 64, p. 137–223.

Weimer, R.J., 1960, Upper Cretaceous stratigraphy, Rocky Mountain area: American Association of Petroleum Geologists, Bulletin, v. 44, p. 1-20.

Willis, B.J., 1997, Architecture of fluvial-dominated valley-fill deposits in the Cretaceous Fall River Formation: Sedimentology, v. 44, p.735-757.

Wright, V.P., and Marriot, S.B., 1993, The sequence stratigraphy of fluvial depositional systems: the role of floodplain sediment storage: Sedimentary Geology, v. 86, p. 203–210.

Wright, A.M., Ratcliffe, K.T., Zaitlin, B.A., Wray, D.S., 2010. The application of chemostratigraphic techniques to distinguish compound incised valleys in low accommodation incised-valley systems in a foreland-basin setting: an example from the Lower Cretaceous Mannville Group and Basal Colorado Sandstone (Colorado Group), Western Canadian Sedimentary Basin, Ratcliffe, K.T., Zaitlin, B.A. eds., Application of Modern Stratigraphic Techniques: Theory and Case Histories: SEPM Special Publication, 94, pp. 93–107.

Zaitlin, B.A., Dalrymple, R.W., and Boyd, R., 1994, The stratigraphic organization of incised-valley systems associated with relative sea-level change, in Dalrymple, R.W., Boyd, R., and Zaitlin, B.A., eds., Incised-Valley Systems, Origin and Sedimentary Sequences: SEPM, Special Publication 51, p. 45–60.

Zhu, Y., 2010, Sequence Stratigraphy and Facies Architecture of the Cretaceous Ferron Notom Delta Complex, Southcentral Utah, USA: PhD Dissertation, University of Houston, Houston, p. 144.

Zhu, Y., Bhattacharya, J.P., Li, W., Lapen, T., Jicha, B.R., Singer, B.S., 2012, Milankovich-scale sequence stratigraphy and stepped forced regressions of the Turonian Ferron Notom Delta Complex, South-Central Utah, U.S.A., Journal of Sedimentary Research, v. 82, p. 723-746.